Comparison of THOR-AV and Volunteer Kinematics during Low-Speed Frontal and Frontal-Oblique Sled Tests

Devon L. Albert, Hana Chan, F. Scott Gayzik, Andrew R. Kemper

Abstract The purpose of this study was to evaluate the kinematic responses of the THOR-AV-05F and THOR-AV-50M to analogously sized volunteers during low-speed frontal and frontal-oblique sled tests. The THOR-AVs and volunteers underwent sled tests in two orientations using two different accelerations pulses (1 g and 2.5 g). The volunteers were tested in each test condition twice: one test in a relaxed muscle state and one test in a braced muscle state. Occupants were instrumented with accelerometer packages at the head and lower neck. Additionally, occupant excursions were measured via a motion capture system. The biofidelity of the THOR-AVs' kinematic responses relative to the volunteers was evaluated using two objective rating metrics. The similarity of the THOR-AV responses to the volunteers varied with test condition, body region, and data type. The biofidelity ranking system scores indicated that the THOR-AVs had good biofidelity (THOR-AV-05F: 1.03; THO-AV-50M: 1.02) when averaged across all body regions and data types. In terms of peak forward excursion, the THOR-AV responses either fell between the responses of the relaxed and braced volunteers, or were less than both responses. Overall, this study found that the THOR-AVs had good biofidelity, but qualitative differences between the THOR-AV and human responses were observed. Future publications will compare the kinetic responses of the volunteers and ATDs as well as compare the responses of the THOR-AV-5F and THOR-AV-50M.

Keywords Autonomous vehicles, biofidelity, Biofidelity Ranking System, ISO/TS 18571, objective rating metric

I. INTRODUCTION

The THOR-AV 50th percentile male and 5th percentile female (THOR-AV-50M, THOR-AV-5F) are anthropomorphic test devices (ATDs) that were introduced as tools to evaluate novel restraint designs associated with the autonomous vehicle (AV) environment [1]. To optimise the THOR-AV ATDs for AV evaluation, several aspects of the THOR ATDs were redesigned [1-2]. The lumbar spine and abdomen were modified to allow the ATDs to recline. Additionally, the neck and pelvis were modified to improve the anatomical biofidelity.

The biofidelity of the THOR-AV-50M responses relative to post-mortem human subjects (PMHS) have already been evaluated in a variety of scenarios including frontal tests in simulated production front and rear seats [3], forward-facing frontal tests with reclined seats [4], and rear-facing frontal tests with upright and reclined seats [1]. For all of these tests, ATD biofidelity was evaluated using the biofidelity ranking system [5], and the resulting scores indicated the THOR-AV-50M had good to excellent biofidelity. However, all of these biofidelity evaluations have been conducted at moderate to high speeds. Increased automation in vehicles, including automated driver assist systems, are intended to prevent crashes and mitigate crash severity. Therefore, lower speed events, such as autonomous braking events or low-speed collisions, may become more prevalent as automation increases.

ATDs must be biofidelic at these speeds in order to accurately predict occupant response. Low-speed ATD biofidelity is assessed using human volunteers instead of PMHS because muscle activation has a larger effect on occupant response at these speeds [6-8]. Previous studies have compared adult and child ATDs to human volunteer responses during low-speed frontal crash or braking events [8-10]. These studies reported the ATDs had lower peak excursions compared to human occupants. With the biofidelity improvements made to the newer THOR-AV ATDs, the THOR-AV-5F and the THOR-AV-50M may be able to better replicate a live human response compared to previous ATDs. Given the design changes and their intended use in the AV environment, there is a need to evaluate the biofidelity of the newer THOR-AVs during lower severity crash and braking events. To meet

D. L. Albert (e-mail: dla16@vt.edu; tel: +1-540-231-1890) is a Research Assistant Professor, H. Chan is a PhD student, and A. R. Kemper is an Associate Professor in the Center for Injury Biomechanics (CIB) at Virginia Tech in Blacksburg, VA, USA. F. S. Gayzik is a Professor in the Center for Injury Biomechanics at the Wake Forest University School of Medicine in Winston-Salem, NC, USA.

this need, the objective of this study was to evaluate the kinematic responses of the THOR-AV-05F and THOR-AV-50M to analogously sized volunteers during low-speed frontal and frontal-oblique sled tests.

II. METHODS

Matched sled tests were performed between the THOR-AV ATDs and human volunteers. To match the THOR-AV-5F, 10 female volunteers aged 19 to 27 years (avg. 22.8 ± 2.7 years) and approximately 5th percentile in height and weight (height: 156.6 ± 4.8 cm; weight: 50.6 ± 2.4 kg) were tested. To match the THOR-AV-50M, 10 male volunteers aged 21 to 26 years (avg. 23.2 ± 2.0 years) and approximately 50th percentile in height and weight (height: 176.2 ± 2.1 cm; weight: 76.4 ± 3.8 kg) were tested. Volunteer testing was approved by the Virginia Tech Institutional Review Board, USA, and each volunteer signed an informed consent form at the start of each test day. Detailed testing methodologies for the volunteer tests have been previously published [11-15].

The volunteers and ATDs were positioned in a rigid test buck of previously reported dimensions [14]. The buck consisted of a seat pan, seat back, left and right foot supports, a steering column with a simulated steering wheel, and United States driver-side three-point seatbelt. The seatbelt was from a model year 2007-2011 Toyota Camry, and had a locking retractor and 3 kN load limiter. However, the load limiter did not engage for any of the tests. The buck was instrumented with load cells at each buck-occupant interface to measure reaction forces and moments. The reaction loads will be compared between the ATDs and volunteers in a future publication. The buck was originally designed for the midsize male anthropometry so spacers were installed at each buck-occupant interface to accommodate the small female anthropometry [14]. Efforts were made to position the volunteers and ATDs in a similar manner by matching the ATD joint angles to the volunteer joint angles as closely as possible.

Each occupant underwent sled tests in four different configurations based on the orientation of the buck and severity of the sled pulse (Fig. 1). The buck was oriented such that occupants experienced either a frontal test (principal direction of force (PDOF) = 0°) or a frontal-oblique test (PDOF = 330°) (Fig. 2). Within each orientation, occupants experienced two acceleration pulses. The first pulse, which was designed to simulate an autonomous braking event, was longer duration with a peak acceleration of approximately 1 g (Fig. 3, left). The second pulse was designed to simulate a low severity crash, and was shorter in duration with a peak acceleration of approximately 2.5 g (Fig. 3, right). Each ATD underwent three tests per combination of orientation and pulse for a total of 12 tests per ATD. Each volunteer underwent two tests per combination of orientation and pulse. One test was in a relaxed state, where the volunteers were distracted by visual and auditory media playing on a TV monitor and were unaware of when the test would begin. During the other test, the volunteers were instructed to brace using their arms and legs in anticipation of the beginning of the test. Accordingly, the subjects were given a countdown to when the test would begin, and were instructed to begin bracing 2 s prior to the test. Therefore, each volunteer underwent a total of 8 tests, producing 80 volunteer tests total.

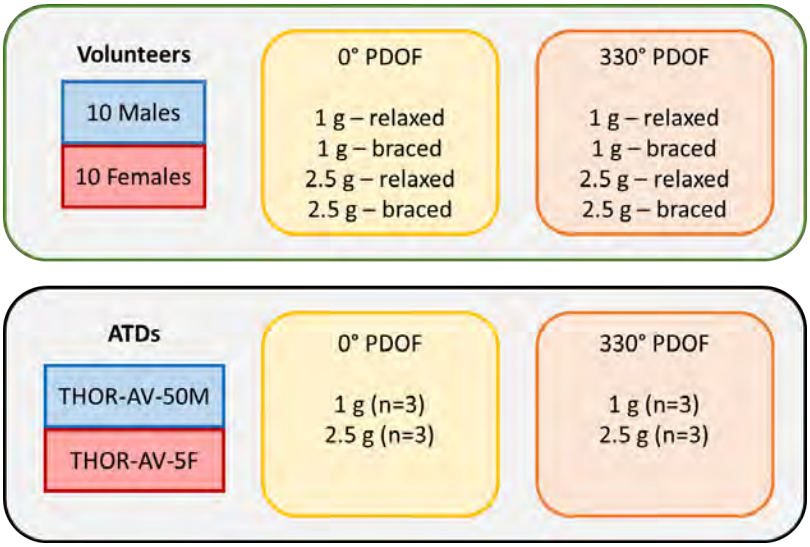

Fig. 1. Test summary diagram for volunteers and ATDs.

Instrumentation and Data Processing

Occupant kinematics were measured using a Vicon motion capture system (Vicon Motion Systems, Oxford, United Kingdom), accelerometers, and angular rate sensors. Retroreflective markers were adhered to the occupants and sled buck via tape at key anatomical locations. Regions of interest included the head centre of gravity (CG),

shoulders, elbows, hips, and knees, bilaterally. The left and right head CG markers were averaged to obtain the position of a central head CG location. Certain markers near the belt path were occasionally removed from the volunteers prior to a test to prevent contact with the belt. These markers and other markers that became obstructed during the test were reconstructed via rigid body mechanics from static capture data collected prior to testing. The 3D coordinates of the markers were collected at 1000 Hz in a coordinate system aligned with the test buck and SAE J211 (Fig. 1) [16]. The trajectories of the locations of interest relative to the test buck were calculated by subtracting the motion of the buck. Forward (+x), lateral (+y, right), and vertical (+z, down) excursions were then calculated by subtracting the initial position of each marker from its trajectory time history.

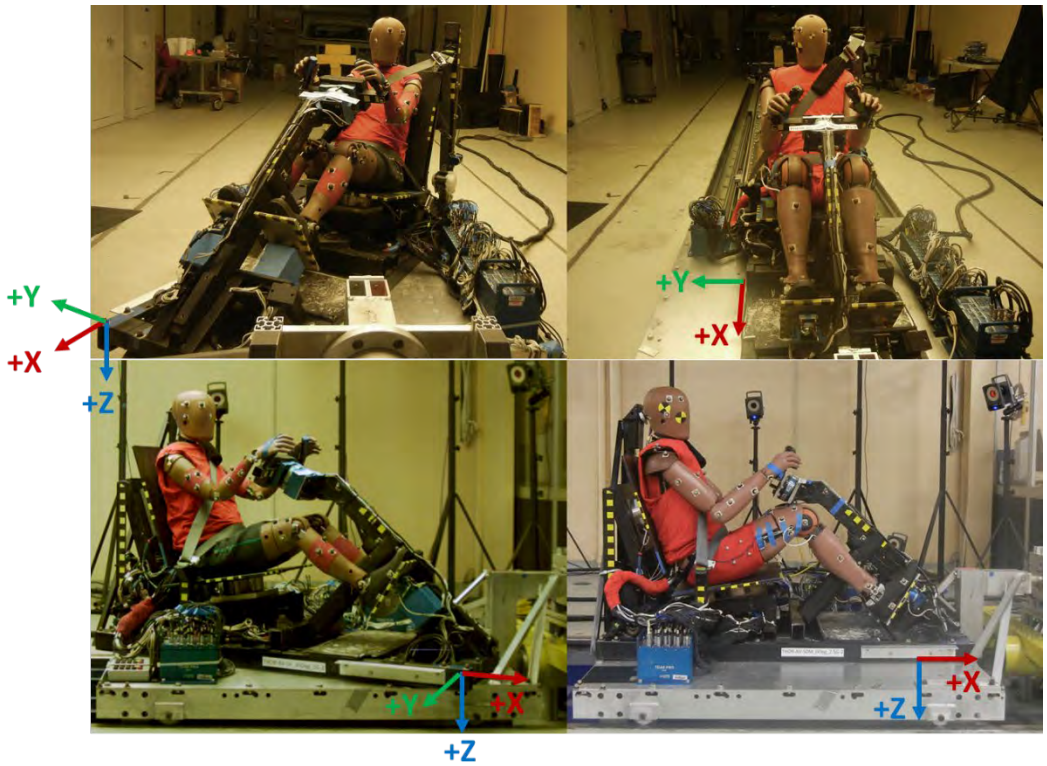

Fig. 2. Test buck in frontal-oblique orientation with the THOR-AV-5F (left) and frontal orientation with the THOR-AV-50M (right). The buck coordinate system is indicated for both orientations.

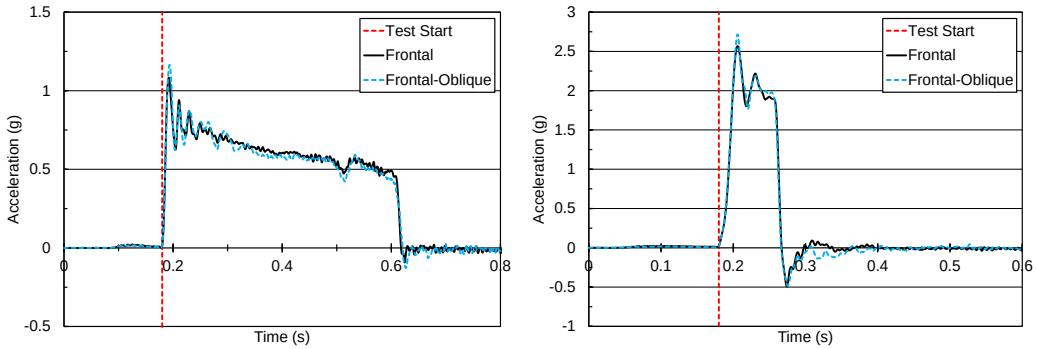

Fig. 3. Sled acceleration time histories for the 1 g (left) and 2.5 g (right) pulse severities.

The volunteers and ATDs were instrumented with analogous accelerometer packages on the head and lower cervical spine/upper thoracic spine. For the volunteers' head instrumentation, a six degree of freedom (DOF) motion block (6DX-Pro, DTS, Seal Beach, CA, USA) was rigidly mounted to a dental tray. Prior to testing, a thermoplastic mouthguard was molded to the upper and lower teeth of each volunteer. Before each test, the volunteers placed the mouthguards over their teeth and the instrumented dental tray was centered inside their mouths. The volunteers were instructed to bite firmly on the mouthguard and wore a custom chinstrap to keep their jaws closed. Prior to each test, lateral pictures were taken to record the location of the motion block relative to the auditory meatus, which was used to approximate the head CG. During data processing, these distances were used to transform the linear accelerations from the mouthguard to the approximate location of the head

CG using rigid body dynamics [17]. The volunteers were also instrumented with a 3-DOF motion block at the seventh cervical vertebra (C7). The motion block consisted of three linear accelerometers (7264C, Endevco, Halifax, NC, USA). The block was glued to an adhesive patch, which was then adhered to the subject's skin over the C7 spinous process. Each ATD was instrumented with a 6 DOF motion block at the head CG consisting of three linear accelerometers (7264C, Endevco, Halifax, NC, USA) and three angular rate sensors (ARS PRO-18K, DTS, Seal Beach, CA, USA). The ATDs also had a 3 DOF motion block consisting of three linear accelerometers (7264C, Endevco, Halifax, NC, USA) at the level of the first thoracic vertebra (T1). Due to their analogous locations, the volunteer C7 accelerations were compared to the ATD T1 accelerations.

ATD and volunteer data were recorded using an onboard data acquisition system (TDAS PRO, DTS, Seal Beach, CA, USA) at 20 kHz. Accelerations and angular rates were zeroed using the pre-trigger period, when the volunteers were sitting in a relaxed manner prior to any bracing. Volunteer accelerations were filtered at channel frequency class (CFC) 60, and angular rates were filtered at CFC 12 [16]. ATD accelerations were filtered at CFC 180, and angular rates were filtered at CFC 30. All data were time-aligned such that the beginning of the test occurred at t = 0.18 s. Other data were collected for both the volunteer and ATD tests. Previous publications have reported subsets of the volunteer data [11-13]. Future publications will present the additional ATD data.

Corridor and Objective Rating Metric Calculations

ATD excursions, accelerations, and angular velocities were qualitatively and quantitatively compared to the analogous relaxed and braced volunteer corridors. Corridors were separately calculated for the relaxed and braced volunteer data. Since the data were already time-aligned, the average curve for each volunteer demographic was calculated by computing the mean response across all 10 volunteers at each time point. The standard deviation corridors were calculated in a similar manner by computing the standard deviation at each time point then adding and subtracting the time-dependent standard deviation to the average curves. The ATD responses were then compared to the volunteer average and corridor responses. During four conditions, markers on the ATDs were obscured before the end of the event. As a result, the excursions were truncated and excluded from the objective rating metric analysis. These cases included the left knee excursions for the THOR-AV-50M during the 0° condition for both pulses and the 330° condition for the 1 g pulse, as well as the right hip excursion for the THOR-AV-5F during the 330° condition and 1 g pulse.

The similarity between the ATD and volunteer responses were quantitatively assessed using two objective rating metrics. First, the Biofidelity Ranking System (BRS) was used to assess the biofidelity of the ATDs [5] since this metric has commonly been used to assess the biofidelity of the THOR-AV-50M and other THOR models [2-5][18-21]. The BRS score ranges from zero to positive infinity and is intended to represent how many standard deviations the ATD response is from the average human response. Therefore, a lower score indicates better biofidelity. In the current version of BRS, the score is optimised by shifting the ATD curve relative to the human response until the BRS is minimised. Then both the BRS score and the size of the phase shift are reported. For this study, large phase shifts (>0.1 s) were observed for some responses, and BRS scores represented the comparison between dissimilar phases of the ATD and volunteer responses. It was difficult to identify and impose a phase shift limit because responses were already time-aligned based on sled acceleration, and there was no volunteer phase shift for context. Therefore, the phase shift was eliminated from the calculation, and all BRS scores were calculated based on the natural alignment of the data based on the sled pulse. To compensate for this modification, a second objective rating metric, defined by the International Organization for Standardization (ISO) in Technical Specification 18571, was calculated [22]. The ISO metric computes corridor, phase, magnitude, and slope scores, which are then combined into a single score (ISO score). The score ranges from 0 (not at all similar) to 1 (perfect similarity). Scores can also be evaluated on a qualitative scale of excellent (>0.94), good (>0.80 & <0.94), fair (>0.58 & <0.80), and poor (<0.58). This is a similarity scale that does not directly correlate to biofidelity.

Both objective rating metrics required that responses were limited to the relevant region of the time history curve. For this study, the volunteer and ATD responses were truncated to the region of interest using the CORA truncation algorithm [23]. If pre- or post-event data still remained after running the algorithm, the curves were manually truncated to begin no earlier than t = 0.18 s and end no later than t = 0.62 s. After truncation, the BRS and ISO scores were calculated for all 36 signals by comparing the ATD responses to both the relaxed and braced volunteer responses for all four orientation and pulse combinations. The scores were calculated separately for each of the three ATD tests per condition, then the resulting scores were averaged to produce a singular score for that response and condition. This produced a total of 288 scores for each ATD and each rating metric.

III. RESULTS

Qualitatively assessing the THOR-AV-5F and THOR-AV-50M relative to the responses of the male and female volunteers indicated that the similarity between the ATD and volunteer responses varied with test condition, body region, and whether the volunteers were braced or relaxed. Due to the large number of signals and test conditions evaluated, amounting to 288 graphs, graphs of all signals and test conditions could not be included Therefore, graphs of exemplar test conditions were included to support observations made in the text. In general, the THOR-AV-5F and THOR-AV-50M followed the same trends regarding how well they replicated the volunteer responses. At the C7/T1 location for both PDOFs, minimal acceleration was observed for the 1 g pulse for both the ATDs and volunteers, so their responses were similar. For the 2.5 g pulse, the ATDs tended to match the accelerations of the relaxed volunteers better than the braced volunteers (Fig. 4).

At the head, the ATD X accelerations reasonably matched those of the volunteers for the 1 g pulse. However, the ATD peak accelerations were larger than the volunteer accelerations for the 2.5 g pulse (Fig. 5). These observations were true for both PDOFs. For head angular velocity about the Y axis, the ATD responses were most similar to the responses of the braced volunteers (Fig. 6). Differences were also observed between the ATD and volunteer forward and vertical head excursions. For both PDOFs, the heads of the relaxed volunteers first moved forward, then started to move downward as well. When braced, volunteers moved both forward and down immediately (Fig. 7 and Fig. A1). Peak forward excursion decreased when volunteers were braced. In the frontal orientation, the ATDs had less downward excursion than the volunteers, regardless of pulse or bracing state. For the frontal 1g pulse, the ATDs also had less forward excursion than the volunteers, regardless of bracing state. For the 2.5 g pulse, the ATD heads moved farther forward than the braced volunteers, but not as far as the relaxed volunteers. In other words, the ATD response fell between the responses of the relaxed and braced volunteers. In the frontal-oblique orientation, how well the ATDs matched the volunteer response was less consistent (Fig. A1).

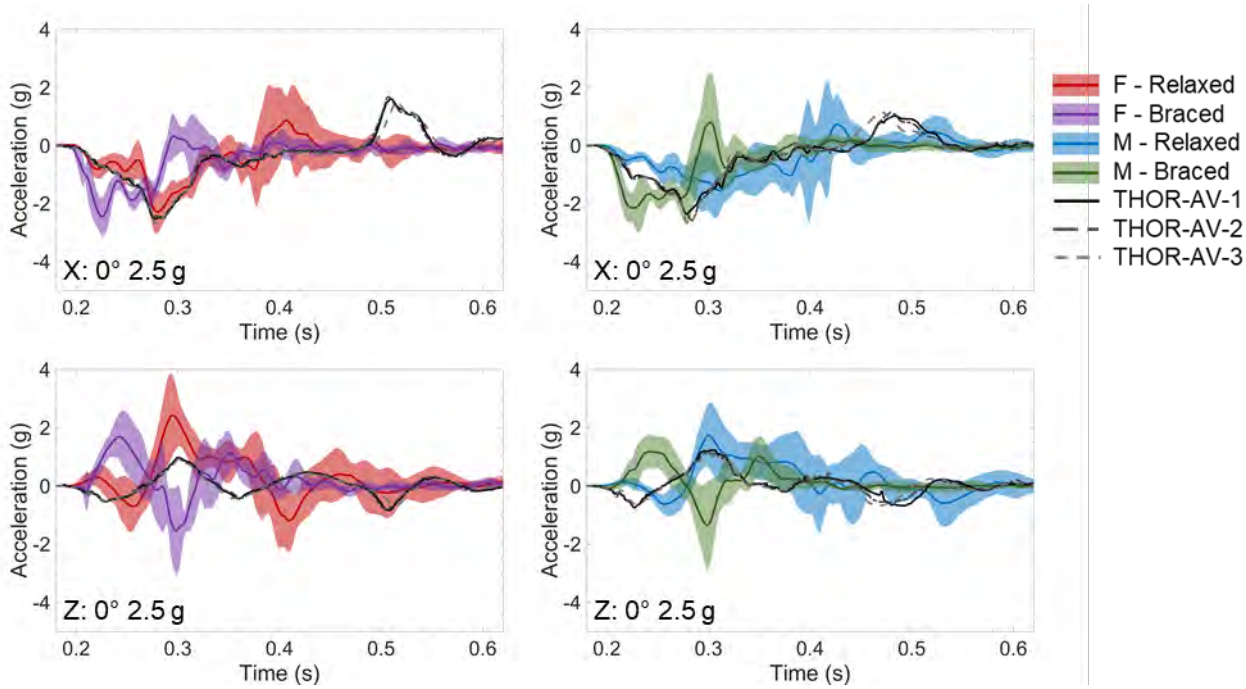

Fig. 4. C7/T1 X (top) and Z (bottom) accelerations for the frontal 2.5 g condition.

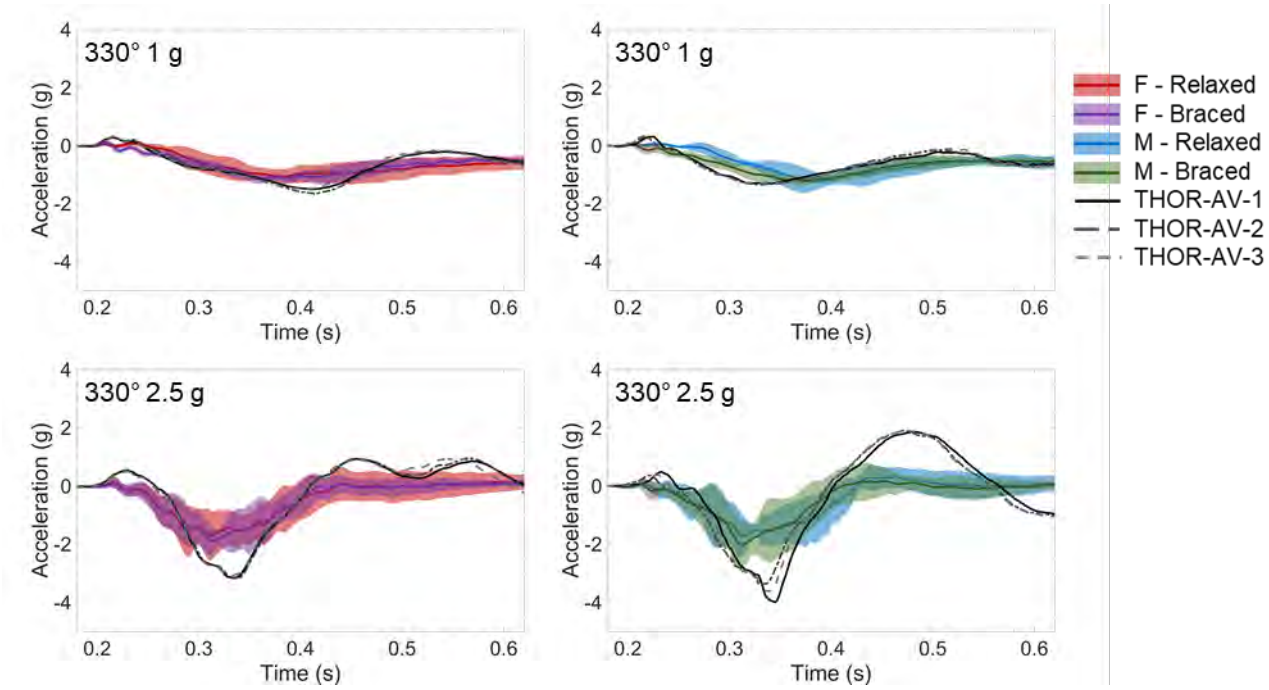

Fig. 5. Head X accelerations for the frontal-oblique 1g (top) and 2.5 g (bottom) conditions.

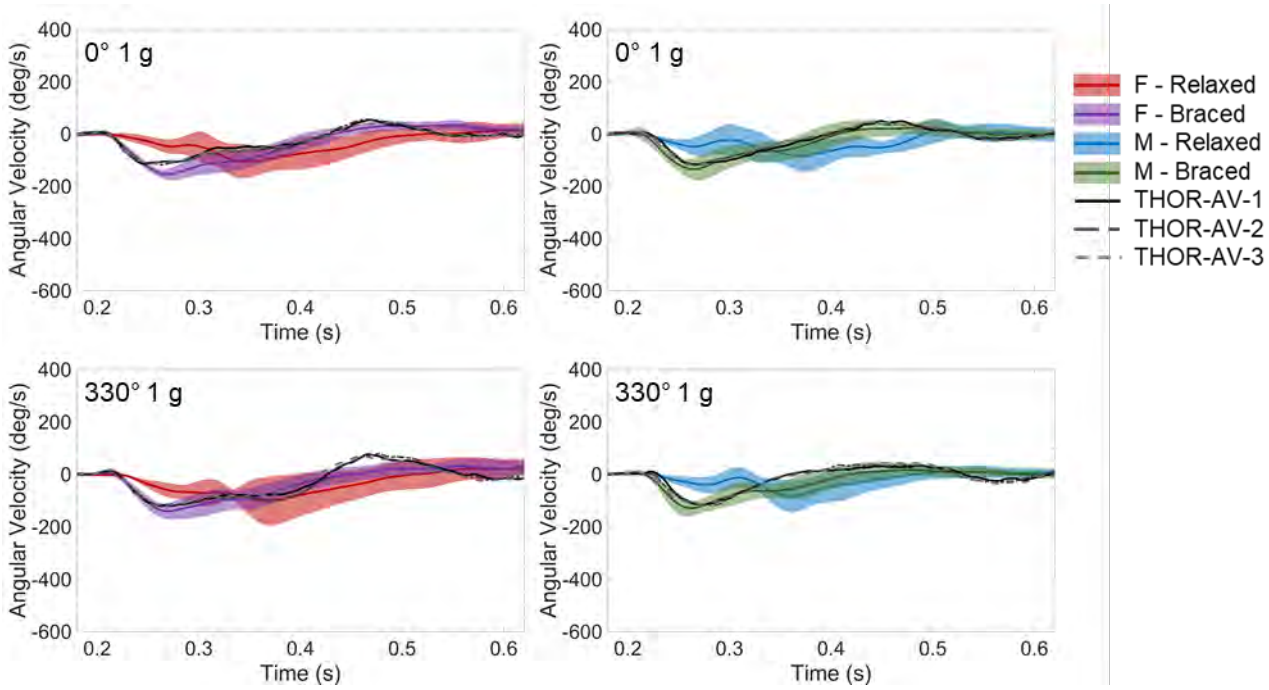

Fig. 6. Head Y angular velocities for the 1 g condition.

For the response at the shoulder, the volunteers had greater forward excursions when relaxed than when braced. The ATD excursions tended to be closer in magnitude to the relaxed volunteer responses. Depending on the specific test condition, the ATDs either had larger forward excursions than the volunteers, matched the relaxed response, or fell between the relaxed and braced excursions (Fig. 8 and Fig. A2). Part of this observed variability in responses may be due to the ATD responses during the frontal-oblique tests. In this orientation, the ATDs' left shoulders moved farther forward than their right shoulders (Fig. 8). This left/right difference was absent in the volunteer shoulder excursions. For the ATDs, this phenomenon propagated to the elbows (Fig. 9). In fact, the THOR-AV-50M right elbow actually moved backward as if the ATD was twisting around the Z axis. It should be noted that both hands remained engaged with the steering handles throughout the tests. There may be a similar motion in the volunteer elbow excursions. However, the trend, if present, is much smaller and more difficult to discern. This twist observed in the ATD shoulders and elbows does not seem to fully propagate to the hip (Fig. 10). A small trend may still be present, but again, it is smaller and difficult to discern.

At the hips and knees, the volunteers moved farther forward when relaxed compared to braced for both orientations (Fig. 10 and Fig. 11). For the 1 g pulse, the ATDs had minimal forward excursion and did not move as far as the volunteers regardless of muscle state. However, the ATD response was comparable to the braced volunteer response for some cases with the 2.5 g pulse.

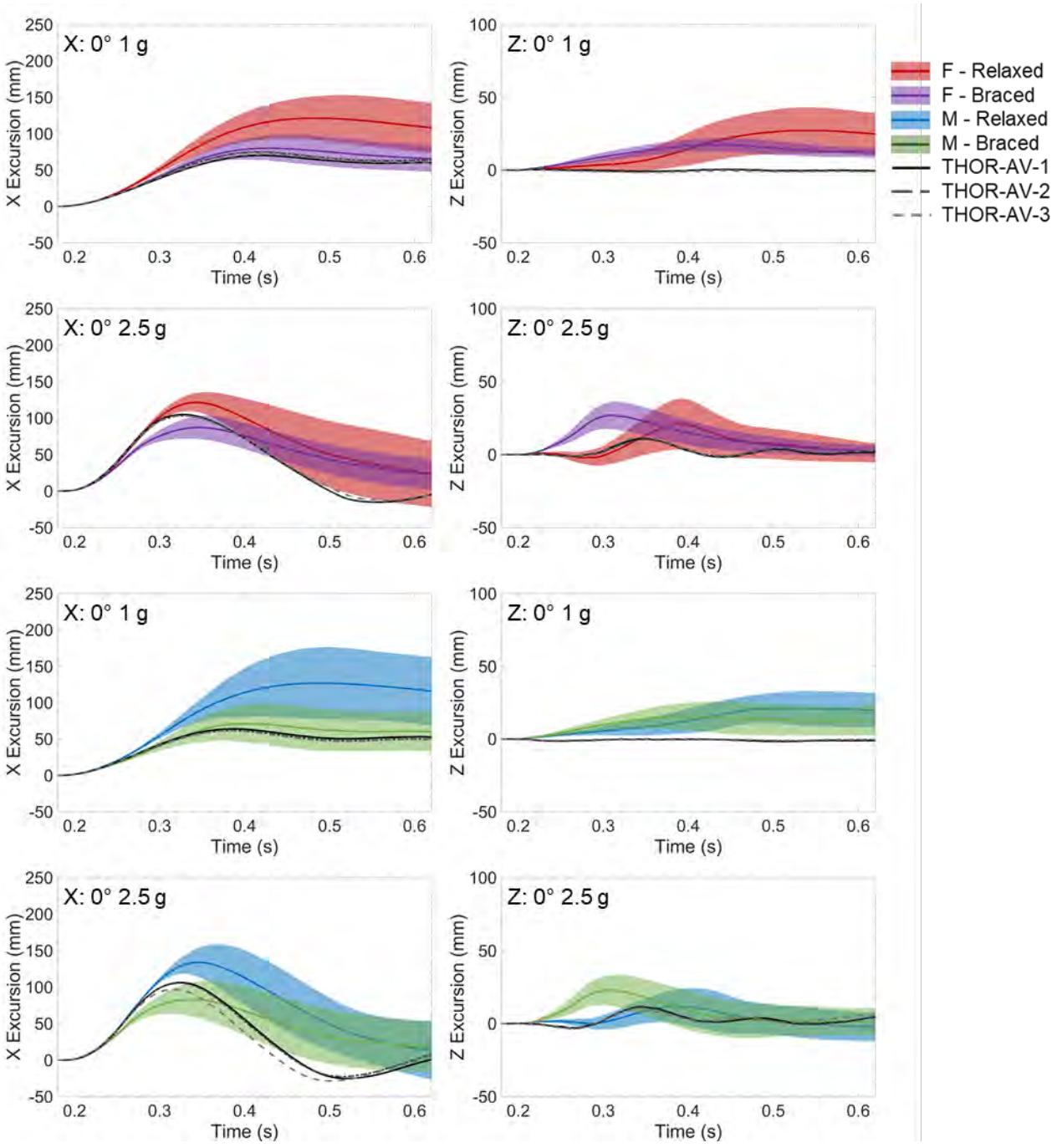

Fig. 7. Head X (left) and Z (right) excursions for all frontal conditions.

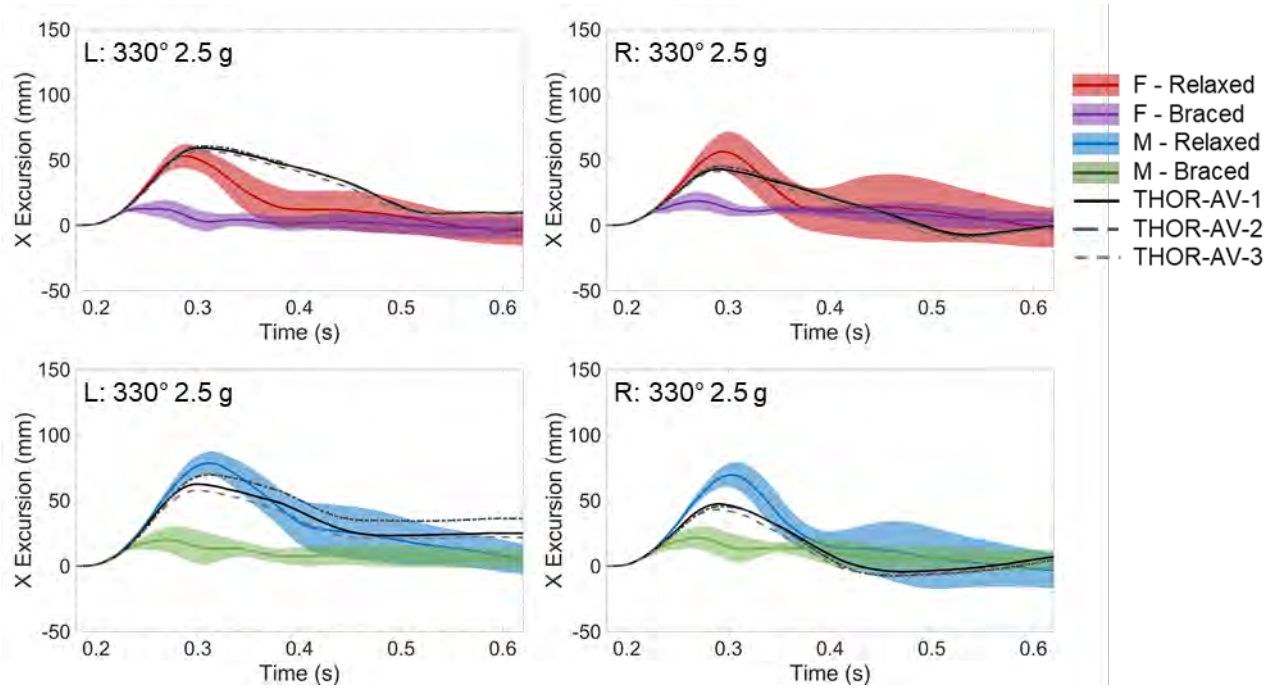

Fig. 8. Left (left) and right (right) shoulder forward excursions for the frontal-oblique 2.5 g condition.

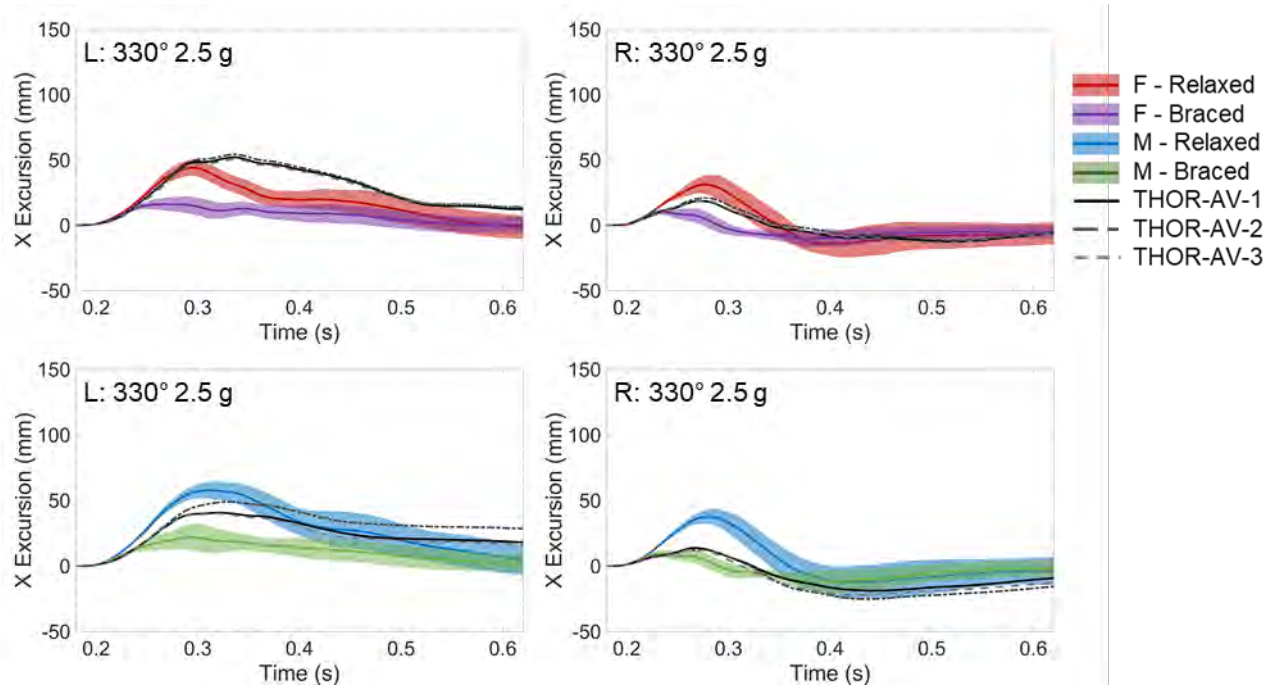

Fig. 9. Left (left) and right (right) elbow forward excursions for the frontal-oblique 2.5 g condition.

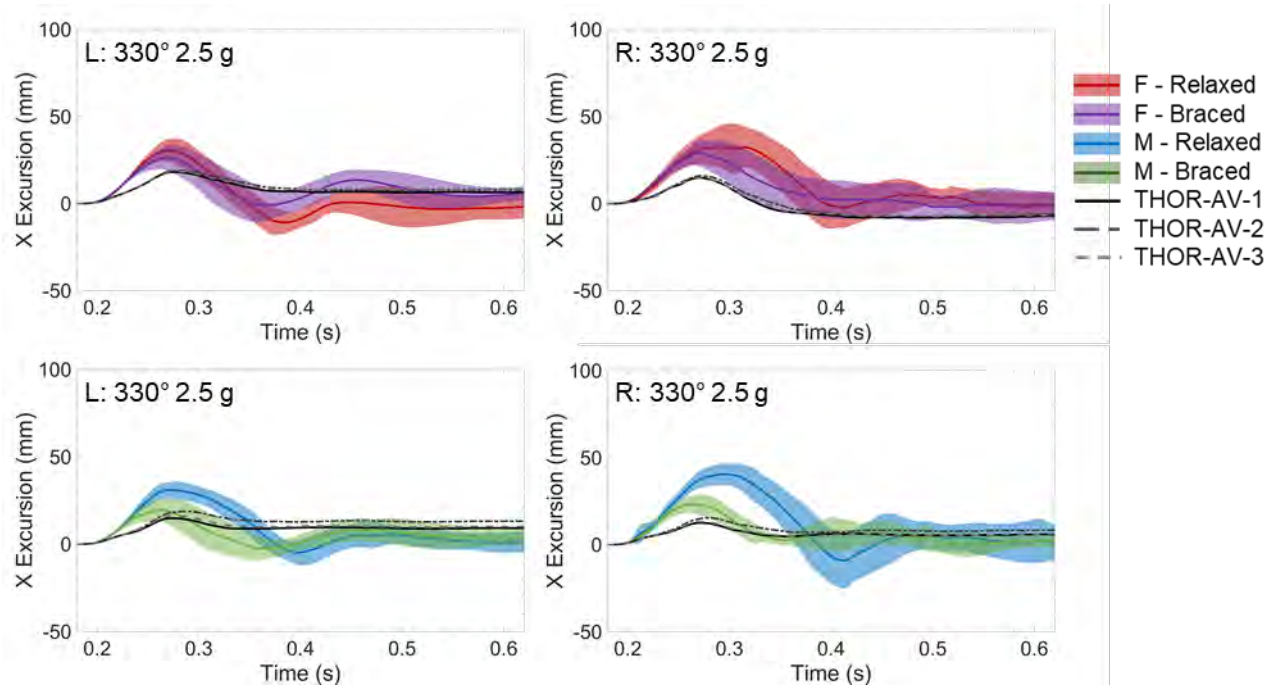

Fig. 10. Left (left) and right (right) hip forward excursions for the frontal-oblique 2.5 g condition.

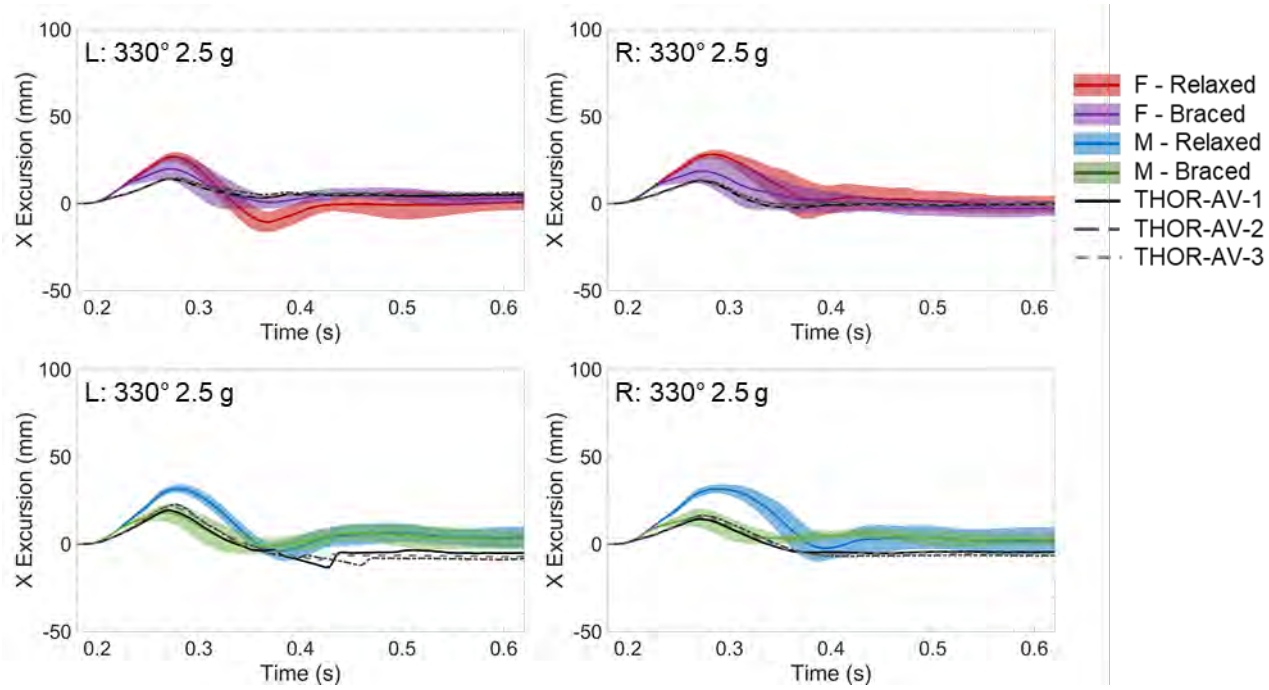

Fig. 11. Left (left) and right (right) knee forward excursions for the frontal-oblique 2.5 g condition.

When comparing responses between the left and right sides of the body for the frontal-oblique orientation, an interesting phenomenon was observed. The ATDs' left shoulders and elbows moved downward, while their right shoulders and elbows moved upward (Fig. 12 and Fig. 13). This movement did not propagate to the hips or knees (Fig. 14 and Fig. 15). Hence, the ATD torso was flexing left and down about the -X axis in addition to the rotation about the +Z axis described above for the frontal-oblique orientation. Evidence of this tilt was also observed in the head angular rate responses, where the ATDs had a greater negative magnitude than the volunteers (Fig. 16). This -X rotation was not observed in the volunteers' upper body responses, but similar movement was observed in the volunteer hips and knees. The volunteers' left lower extremities moved downward, while their right lower extremities moved upward. Based on these observations, the ATDs and volunteers responded to the obliquely-oriented acceleration differently. The volunteer lower extremities tilted, while their upper bodies did not. Conversely, the ATDs lower extremities remained flat on the seat pan, while their upper bodies tilted.

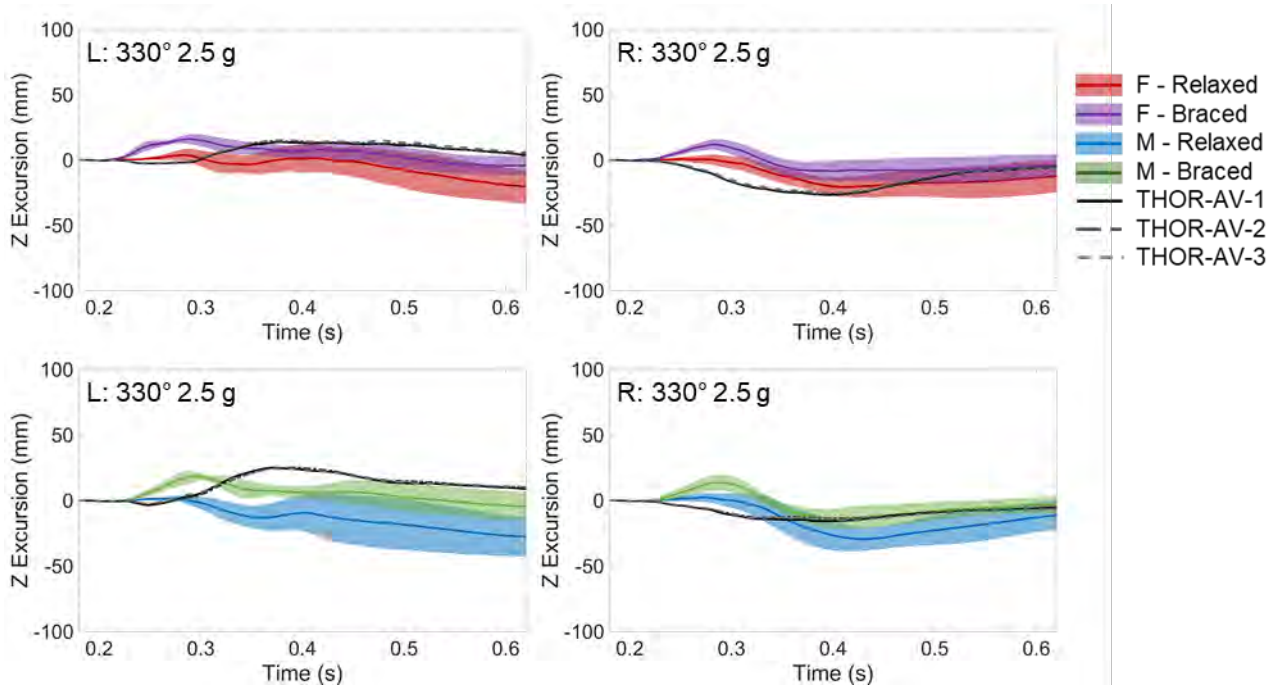

Fig. 12. Left (left) and right (right) shoulder vertical excursions for the frontal-oblique 2.5 g condition.

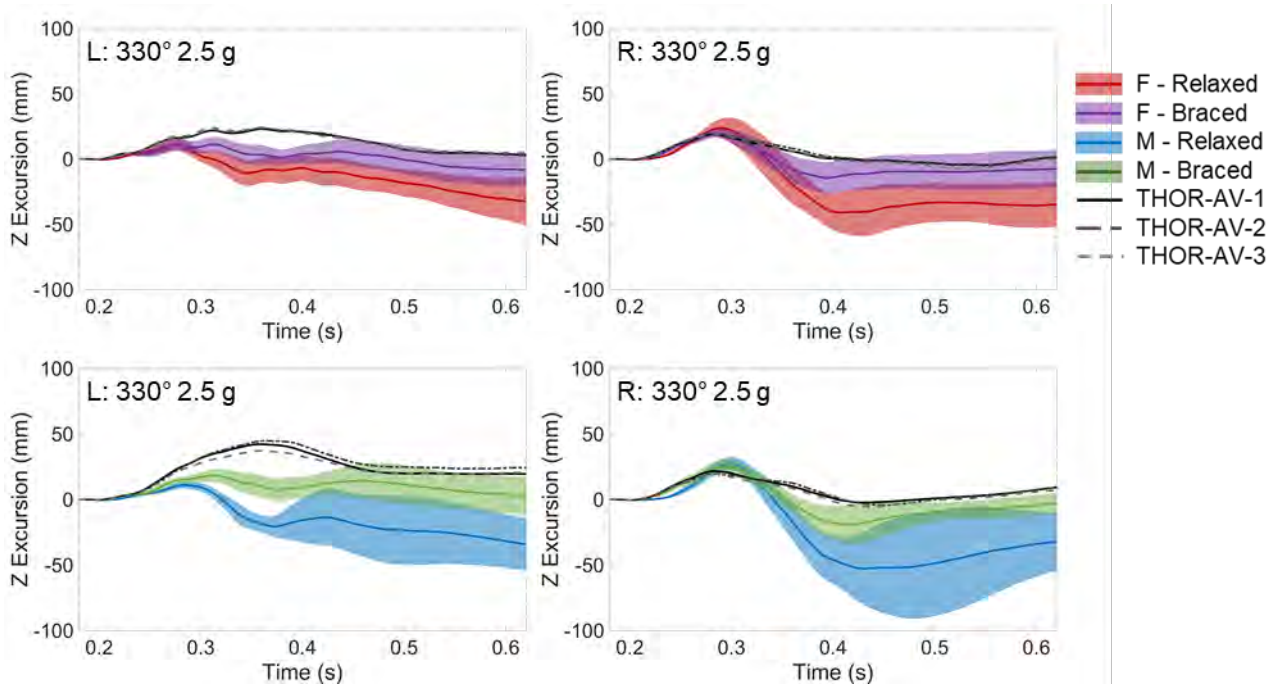

Fig. 13. Left (left) and right (right) elbow vertical excursions for the frontal-oblique 2.5 g condition.

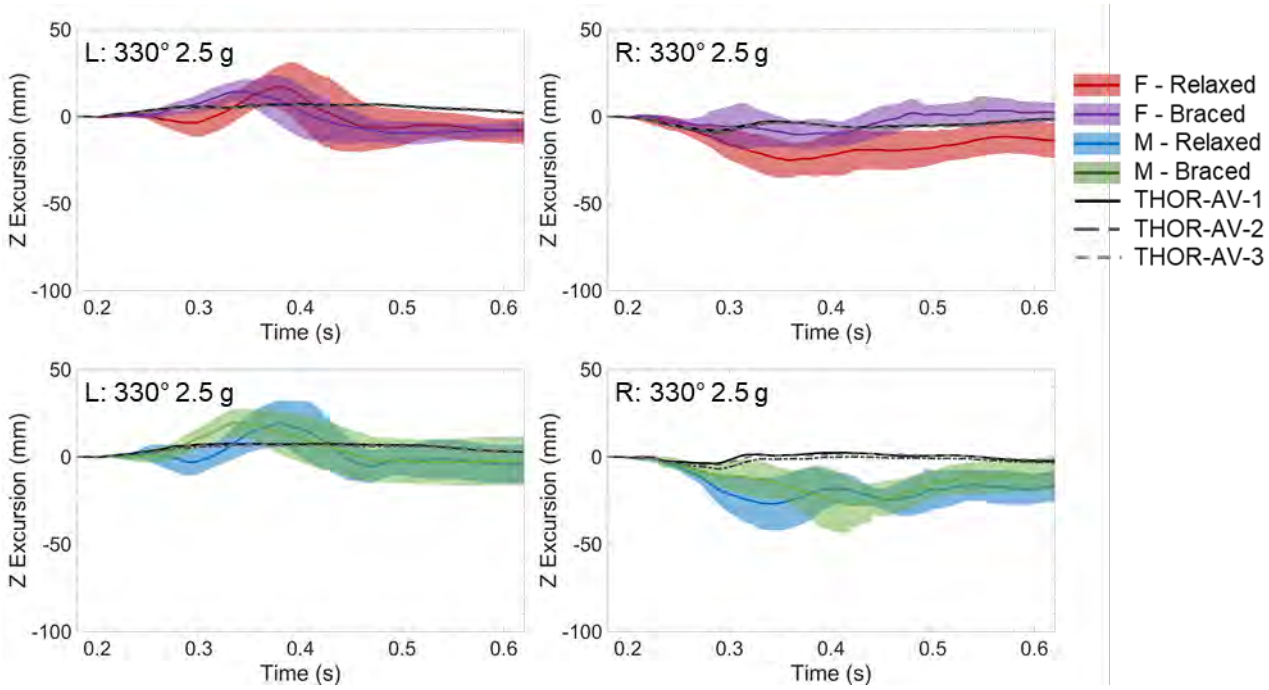

Fig. 14. Left (left) and right (right) hip vertical excursions for the frontal-oblique 2.5 g condition.

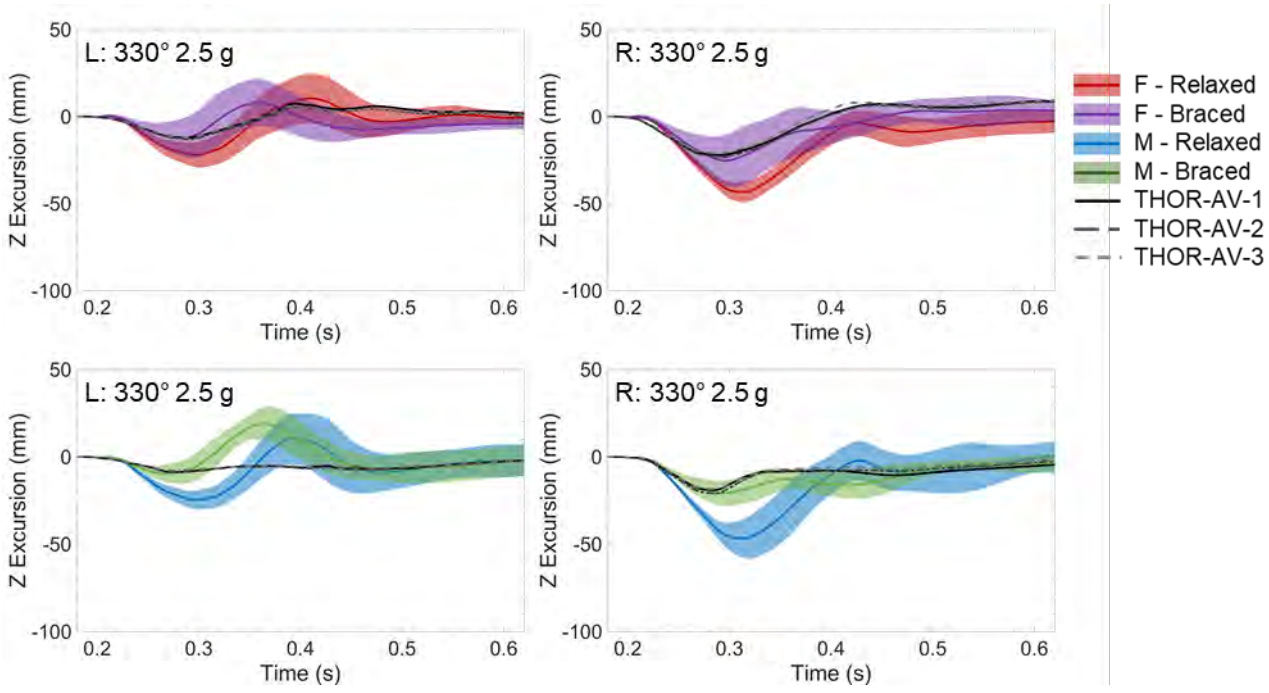

Fig. 15. Left (left) and right (right) knee vertical excursions for the frontal-oblique 2.5 g condition.

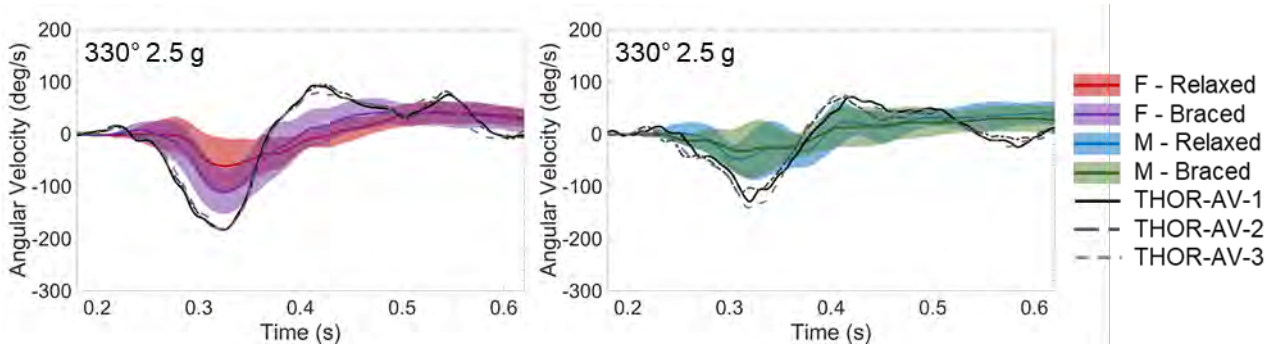

Fig. 16. Head angular velocities around the X axis for the frontal-oblique 2.5 g condition.

To evaluate the biofidelity of the ATD responses relative to the volunteer responses, BRS scores were calculated (Table I, and Tables AI-AII in the Appendix). BRS scores less than 2 indicate good biofidelity. Averaging the BRS scores across all conditions and responses for each ATD showed that the THOR-AV-5F and THOR-AV-50M had similar biofidelity with scores of 1.03 and 1.02, respectively. BRS scores were then averaged across different body regions/data types to understand how biofidelity varied with respect to these parameters. For both the THOR-AV-5F and THOR-AV-50M, the shoulder excursions had the worst biofidelity, while the C7/T1 accelerations had the best biofidelity.

The ISO metric does not directly assess biofidelity because there are no established thresholds to delineate good versus poor biofidelity. For this study, it was calculated to compare the relative biofidelity between the two ATDs and different body regions/data types. In accordance with the BRS scores, the ISO scores indicated that the THOR-AV-5F and THOR-AV-50M had a similar level of biofidelity. However, the two metrics did not agree on the relative biofidelities of the different body regions and data types. The head angular rate sensors had the worst ISO scores, but good BRS scores. The ISO scores indicated that the head excursions, head accelerations, and C7/T1 accelerations had the best biofidelity, which agreed with the BRS scores.

TABLE I
BRS AND ISO SCORES AVERAGED PER SIGNAL AND ACROSS ALL SIGNALS.

	Female BRS	Male BRS	Female ISO	Male ISO
Head Angular Rate	1.088	0.952	0.287	0.276
Head Acceleration	1.171	0.983	0.429	0.402
C7/T1 Acceleration	0.822	0.704	0.428	0.467
Head Excursion	1.136	1.134	0.495	0.430
Shoulder Excursion	1.808	1.640	0.355	0.357
Elbow Excursion	1.537	1.561	0.315	0.317
Hip Excursion	0.922	1.221	0.379	0.327
Knee Excursion	1.040	1.276	0.386	0.393
All	**1.031**	**1.022**	**0.386**	**0.375**

IV. DISCUSSION

This study evaluated the kinematic responses of the THOR-AV-5F and THOR-AV-50M ATDs relative to analogous human volunteers during low-speed sled tests. For many body regions and conditions, the ATDs had lower peak excursions compared to the volunteers. Depending on the body region and pulse severity, the ATDs either had lesser excursions compared to both the relaxed and braced volunteers, or the ATD response fell between the relaxed and braced volunteers. In other words, the ATDs moved forward farther than the braced volunteers, but not as far forward as the relaxed volunteers. These results generally agree with previous studies that compared the kinematics of ATDs and human volunteers, which are discussed below.

Previous studies compared children's kinematics with child ATDs in frontal sled tests and sudden braking manoeuvres [9-10]. They observed that the children displaced farther forward than the ATDs. Additionally, [10] reported that the children exhibited larger head rotations than the ATDs.

For the adult population, Beeman *et al.* compared the excursions of the Hybrid III 50th percentile male ATD to approximately 50th percentile male volunteers during low-speed frontal sled tests [8]. The volunteers were tested in both relaxed and braced conditions, similar to the conditions used in the current study. All occupants were tested using the same 2.5 g acceleration pulse used in the current study, as well as a 5 g pulse. Beeman *et al.* reported that the relaxed volunteers displaced farther forward than the Hybrid III across all body regions for both pulses. However, the displacement of the ATD relative to the braced volunteers varied with body region. The ATDs' upper bodies had larger forward excursions than the braced volunteers, while the opposite trend occurred for the lower body. Interestingly, the same region-dependent response was not observed in the current study, despite similar methodologies. In the current study, the forward excursion differences between the THOR-AV ATDs and the volunteers tended to stay consistent across the upper and lower body. Instead, the relative responses of the volunteers and THOR-AVs depended upon pulse severity. With some exceptions, the relaxed and braced volunteers both displaced farther than the ATDs for the 1 g pulse. However, the ATD response typically

fell between the relaxed and braced volunteers for the 2.5 g pulse. These differences between the THOR-AV and Hybrid III responses may be due to differences in ATD design between the Hybrid III and THOR-AV ATDs. Major differences include more anatomically accurate pelvis, abdomen, thorax, shoulder, and neck designs for the THOR-AV ATDs. In particular, the necks of the THOR-AV-5F and THOR-AV50M have been shown to be more biofidelic than their Hybrid III counterparts [20-21].

As the previous studies have discussed, ATD responses are designed to match the human body response during higher velocity and more severe impact conditions than the low-speed conditions used to test human volunteers. This results in ATDs that exhibit a stiffer response than the human body during less severe impact conditions. Hence, volunteers often exhibit greater excursions than ATDs.

The notable exception to this trend was the forward excursion at the shoulder. The THOR-AV forward shoulder excursions were typically more similar to the relaxed volunteers than the braced volunteers. This result was unexpected since the ATDs generally had lesser hip and head forward excursions compared to the volunteers, which would indicate the entire upper body was moving less for the ATDs. While the C7/T1 accelerations were similar between the ATDs and volunteers, no other matched instrumentation was available on the spine for both types of occupant. Therefore, it is not clear whether the spine at this location is moving more biofidelically than the other body regions, or whether the shoulder is over-protracting for the ATDs relative to the volunteers. Greater protraction of the ATD shoulder would allow the shoulders to move farther forward, independent of the lag in the ATD spine forward excursion, producing excursions more similar to the relaxed volunteers.

It is possible that there is some error in the ATD shoulder excursion due to the retroreflective marker placement. The rigid shoulder structure of the THOR-AV ATDs is covered by a skin flap, which is partially secured to the shoulder structure, but still able to move relative to the underlying structure. Superior and medial to the shoulder flap is the edge of the THOR-AV's jacket. The edge of the jacket is more analogous to the acromion on a human, which is where the shoulder markers were located on the human volunteers. However, the jacket is much more mobile relative to the underlying rigid structures of the ATD compared to the shoulder flap. Hence, the shoulder flap was chosen as the more ideal location for the shoulder marker despite the fact that there can be some extraneous motion of the flap. The motion of the flap relative to the shoulder could produce some error in the ATD shoulder excursions, potentially increasing the measured forward excursion compared to the true motion of the underlying structure. However, any effect, if present, is likely to be small at the low-speeds in this study.

As discussed above, frontal ATDs are generally designed to be biofidelic at higher severity tests. Therefore, it can be hypothesized that ATD performance would improve at the higher pulse severity in this study. As discussed above, this was sometimes true when the ATD response was underestimating the volunteer relaxed and braced responses at the lower severity. Increasing the severity from the 1 g to 2.5 g pulse resulted in an ATD response that was between the relaxed and braced volunteer responses. However, there were other cases where the ATD response matched the volunteer responses during the 1 g pulse because responses across all surrogates were minimal in terms of magnitude. In those cases, increasing the pulse severity to 2.5 g produced greater discrepancies between the ATD and volunteer responses relative to the 1 g pulse (Fig. 17).

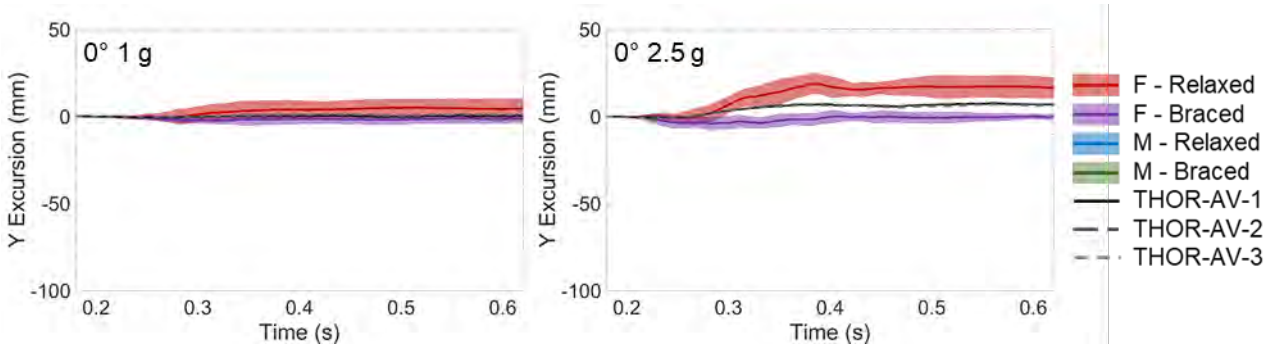

Fig. 17. Left hip lateral excursions for the frontal 1 g (left) and 2.5 g (right) conditions.

Two objective rating metrics were used in this study to assess the biofidelity of the THOR-AVs relative to the volunteers. The BRS scores in this study were limited because the ATD data were not shifted to optimally align with the volunteer data prior to score calculation. Allowing the shift resulted in lower (more biofidelic) scores than those reported in the study. Specifically, allowing a shift decreased the THOR-AV-5F score from 1.03 to 0.84.

The THOR-AV-50M score decreased from 1.02 to 0.82. This would have changed the qualitative ranking of overall biofidelity from good to excellent. These two sets of values could be considered bounds for THOR-AV biofidelity under these conditions. The shifted scores would represent the best possible biofidelity rating, while the unshifted scores would represent the most conservative estimate of biofidelity. Use of the ISO metric was intended to compensate for eliminating the phase shift in the BRS score since the ISO score includes a phase-specific sub-score. In many cases, the comparative biofidelity reported by the BRS scores was supported by the ISO score results. However, the two metrics differed in their scoring of the head angular velocities. The BRS scores indicated good biofidelity, while the ISO scores indicated they were the least biofidelic of all of the body regions/data types. The lower ISO scores were driven by differences in how the magnitude score was calculated between the two metrics. The ISO score does not account for the size of the standard deviation around the mean volunteer response, which can lead to harsher score penalties compared to the BRS calculation.

The qualitative interpretation of the unshifted BRS scores is that the THOR-AV responses fell on the border of the volunteer one standard deviation corridors, on average. Phase shifting the ATD responses relative to the volunteer responses would place the THOR-AV responses inside the volunteer corridors, on average. Therefore, the THOR-AV responses were able to approximate the volunteer responses, but were sometimes out of phase relative to the volunteers. Additionally, the THOR-AV responses did not consistently match either the braced or relaxed muscle state of the volunteers. These two muscle states represent the two extremes of unaware and completely aware and bracing. In a real-world event, it is likely the average human response will lie somewhere between these two states. Since the responses of the THOR-AVs varied in terms of which muscle state they more accurately matched, depending on pulse severity, orientation, and body region, the response of the THOR-AVs may also sit somewhere on the range between the two states.

The results of this study demonstrate that the THOR-AV-5F and THOR-AV-50M were able to match the responses of analogously sized volunteers with good biofidelity under low-speed braking and crash events relevant to the autonomous vehicle environment for which the ATDs were designed. However, this study only evaluated the kinematic data that were available for both the ATDs and volunteers. Other facets of the THOR-AV responses, including kinetics and injury prediction, should be evaluated during low-speed events. Although injuries would not be expected for such low severities, braking events can be precursors to more severe events. Therefore, it is important to assess how biofidelic the THOR-AV responses are across the range of low- and high-severity events.

V. CONCLUSION

The results of this study indicated that both the THOR-AV-5F and THOR-AV-50M had good biofidelity under these test conditions. Furthermore, the THOR-AV-5F and THOR-AV-50M had very similar biofidelity scores, showing they were each able to represent their intended demographic group. In terms of peak forward excursion, the THOR-AV responses either fell between the responses of the relaxed and braced volunteers, or were less than both muscle state responses. An exception was the shoulder forward excursion, where the ATD responses were more similar to the relaxed volunteers. The volunteers and ATDs had slightly different responses to the frontal-oblique PDOF. The volunteers responded to the oblique acceleration by tilting their lower body down on the left side and up on the right side. In contrast, the ATDs exhibited a similar tilt in the upper body instead of the lower body. This analysis was limited to the kinematic responses of the ATDs. Future publications will compare the ATD and volunteer reaction forces as well as other ATD responses.

VI. ACKNOWLEDGEMENTS

The authors would like to thank the volunteers who participated in this study for their time and efforts. The Global Human Body Models Consortium sponsored the volunteer portion of this study. The authors would like to acknowledge Humanetics Innovative Solutions for providing the THOR-AV-5F and THOR-AV-50M.

VII. REFERENCES

[1] Wang, Z.J. (2022) Biomechanical responses of the THOR-AV ATD in rear facing test conditions. *SAE International Journal of Advances and Current Practices in Mobility*, **4**(2022-01-0836): pp. 2089–2105.

[2] Wang, Z.J., Humm, J., Hauschild, H.W. (2023) Investigation of THOR-AV 5F Biofidelity in Sled Test Conditions with a Semi-Rigid Seat. *Stapp Car Crash Journal*, **67**.

[3] Wang, Z.J., Richard, O., *et a*l. (2022) Biomechanical Responses of THOR-AV in a Semi-Rigid Seat that Mimics the Front and Rear Seat of a Midsize Car. *Proceedings of the IRCOBI Conference*, 2022, Porto, Portugal.
[4] Wang, Z.J., Zaseck, L.W., Reed, M.P. (2022) THOR-AV 50th Percentile Male Biofidelity Evaluation in 25 and 45 Seatback Angle Test Conditions with a Semi-Rigid Seat. *Proceedings of the IRCOBI Conference*, 2022, Porto, Portugal.
[5] Hagedorn, A., Stammen, J., *et al*. (2022) Biofidelity Evaluation of THOR-50M in Rear-Facing Seating Configurations Using an Updated Biofidelity Ranking System. *SAE International Journal of Transportation Safety*, **10**(09-10-02-0013)
[6] Beeman, S.M., Kemper, A.R., Duma, S.M. (2016) Neck forces and moments of human volunteers and post mortem human surrogates in low-speed frontal sled tests. *Traffic Injury Prevention*, **17**(sup1): pp. 141–149.
[7] Beeman, S.M., Kemper, A.R., Madigan, M.L., Duma, S.M. (2011) Effects of bracing on human kinematics in low-speed frontal sled tests. *Annals of Biomedical Engineering*, **39**(12): pp. 2998.
[8] Beeman, S.M., Kemper, A.R., Madigan, M.L., Franck, C.T., Loftus, S.C. (2012) Occupant kinematics in low-speed frontal sled tests: Human volunteers, Hybrid III ATD, and PMHS. *Accident Analysis & Prevention*, **47**: pp. 128–139.
[9] Seacrist, T., Mathews, E.A., *et al*. (2012) Kinematic comparison of the hybrid III and Q-series pediatric ATDs to pediatric volunteers in low-speed frontal crashes. *Proceedings of Annals of Advances in Automotive Medicine/Annual Scientific Conference*, 2012, Seattle, WA, USA.
[10] Stockman, I., Bohman, K., Jakobsson, L., Brolin, K. (2013) Kinematics of child volunteers and child anthropomorphic test devices during emergency braking events in real car environment. *Traffic Injury Prevention*, **14**(1): pp. 92–102.
[11] Chan, H., Albert, D., Gayzik, F.S., Kemper, A. (2023) Occupant Kinetics and Muscle Responses of Relaxed and Braced 5th Percentile Female and 50th Percentile Male Volunteers in Low-Speed Frontal Sled Tests. *SAE International journal of transportation safety*, **11**(09-11-03-0012): pp. 1–64.
[12] Chan, H., Albert, D.L., Gayzik, F.S., Kemper, A.R. (2021) Assessment of acclimation of 5th percentile female and 50th percentile male volunteer kinematics in low-speed frontal and frontal-oblique sled tests. *SAE International journal of transportation safety*, **9**(1): pp. 3–103.
[13] Chan, H., Albert, D.L., Gayzik, F.S., Kemper, A.R. (2022) Occupant kinematics of braced 5th percentile female and 50th percentile male volunteers in low-speed frontal and frontal-oblique sled tests. *Proceedings of the IRCOBI Conference*, 2022, Porto, Portugal.
[14] Chan, H., Devane, K.S., Albert, D.L., Gayzik, F.S., Kemper, A.R. (2021) Comparisons of initial joint angles and test buck reaction forces for relaxed and braced 5th percentile female and 50th percentile male volunteers and analogous active human body models in a simulated driver's seat. *Proceedings of the IRCOBI Conference*, 2021, Online.
[15] Albert, D.L., Chan, H., Gayzik, F.S., Kemper, A.R. (2023) Volunteer Bracing Strategies and Variability before Low-Speed Frontal and Frontal-Oblique Sled Tests. *Proceedings of the IRCOBI Conference*, 2023, Cambridge, UK.
[16] SAE (2014) Instrumentation for Impact Test - Part 1 - Electronic Instrumentation, SAE International.
[17] Chan, H. (2023) Occupant Responses of Relaxed and Braced 5th Percentile Female and 50th Percentile Male Volunters during Low-Speed Frontal and Frontal-Oblique Sled Tests, *Dissertation*, Virginia Tech.
[18] Parent, D., Craig, M., Moorhouse, K. (2017) Biofidelity Evaluation of the THOR and Hybrid III 50th Percentile Male Frontal Impact Anthropomorphic Test Devices. *Stapp Car Crash Journal*, **61**: pp. 227–276.
[19] Somasundaram, K., Hauschild, H., *et al*. (2023) THOR-05F biofidelity evaluation in reclined and upright seated postures subjected to frontal crash pulses. *Accident Analysis & Prevention*, **191**: pp. 107185.
[20] Wang, Z.J., Loeber, B., Tesny, A., Hu, G., Kang, Y.S. (2021) Neck biofidelity comparison of THOR-AV, THOR and Hybrid III 50th dummies. *Proceedings of the IRCOBI Conference*, 2021, Online.
[21] Wang, Z.J., Loeber, B.H., Tesny, A., Kang, Y.S. (2023) Biomechanical Responses of a New Neck For THOR-AV 5th Percentile Female Dummy. *Proceedings of the IRCOBI Conference*, 2023, Cambridge, UK.
[22] ISO (2014), Road vehicles - Objective rating metric for non-ambiguous signals, ISO.
[23] Thunert, C. (2017) CORAplus Release 4.0. 4 User's Manual. *PDB (Partnership for Dummy Technology Biomechanics), Gaimersheim, Germany*.

VIII. APPENDIX

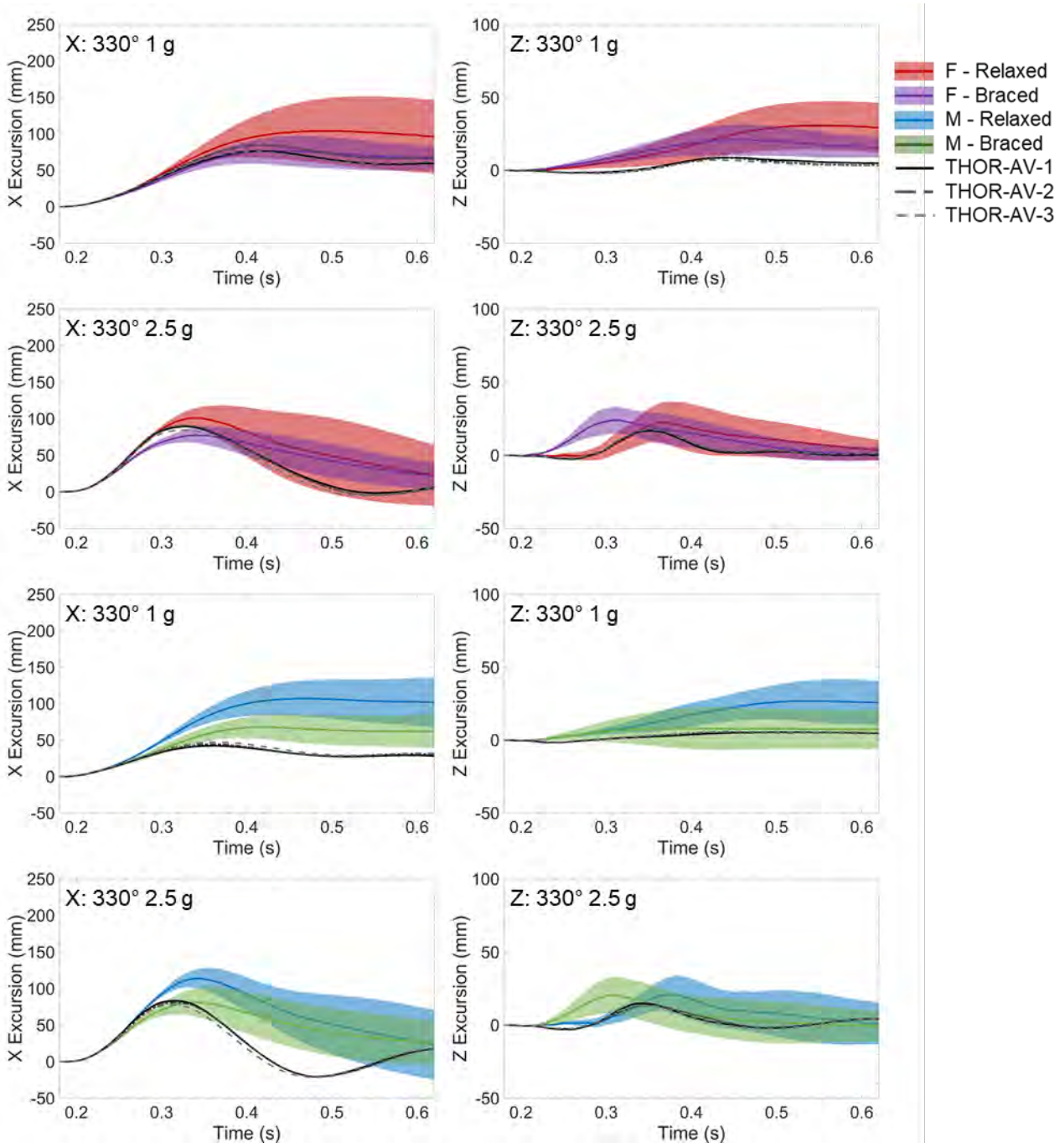

Fig. A1. Head X (left) and Z (right) excursions for all frontal-oblique conditions.

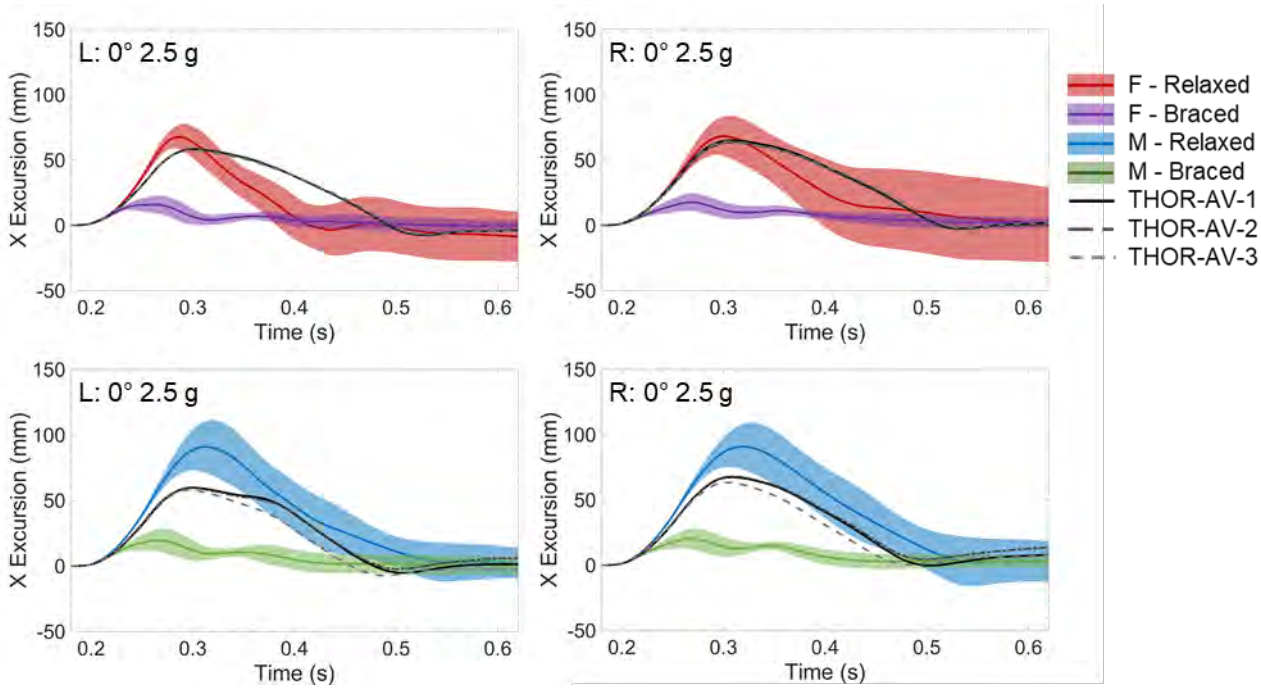

Fig. A2. Left (left) and right (right) shoulder forward excursions for the frontal 2.5 g condition.

TABLE AI

BRS AND ISO SCORES FOR ALL ACCELERATIONS AND ANGULAR RATES.

Muscle Tone	PDOF (°)	Pulse (g)	Location	Signal	Direction	Female BRS	Male BRS	Female ISO	Male ISO
R	0	1	Head	Ang. Vel.	X	0.385	0.596	0.113	0.128
R	0	1	Head	Ang. Vel.	Y	1.064	1.129	0.304	0.278
R	0	1	Head	Ang. Vel.	Z	0.768	0.779	0.184	0.161
R	0	1	Head	Lin. Acc.	X	1.092	1.112	0.536	0.482
R	0	1	Head	Lin. Acc.	Y	0.554	0.387	0.208	0.334
R	0	1	Head	Lin. Acc.	Z	1.113	0.695	0.383	0.315
R	0	1	C7/T1	Lin. Acc.	X	0.858	0.551	0.638	0.697
R	0	1	C7/T1	Lin. Acc.	Y	0.380	0.414	0.191	0.183
R	0	1	C7/T1	Lin. Acc.	Z	1.644	1.156	0.245	0.210
R	0	2.5	Head	Ang. Vel.	X	1.000	0.871	0.159	0.168
R	0	2.5	Head	Ang. Vel.	Y	2.082	2.039	0.305	0.175
R	0	2.5	Head	Ang. Vel.	Z	0.890	0.519	0.130	0.216
R	0	2.5	Head	Lin. Acc.	X	1.994	1.532	0.406	0.342
R	0	2.5	Head	Lin. Acc.	Y	0.918	0.710	0.444	0.366
R	0	2.5	Head	Lin. Acc.	Z	0.908	0.939	0.643	0.477
R	0	2.5	C7/T1	Lin. Acc.	X	0.612	0.806	0.646	0.476
R	0	2.5	C7/T1	Lin. Acc.	Y	0.306	0.471	0.283	0.299
R	0	2.5	C7/T1	Lin. Acc.	Z	0.848	0.747	0.488	0.491
R	330	1	Head	Ang. Vel.	X	1.930	1.203	0.360	0.108
R	330	1	Head	Ang. Vel.	Y	0.850	1.370	0.328	0.211
R	330	1	Head	Ang. Vel.	Z	0.327	0.305	0.327	0.331
R	330	1	Head	Lin. Acc.	X	0.986	1.367	0.442	0.480
R	330	1	Head	Lin. Acc.	Y	1.726	0.760	0.343	0.565
R	330	1	Head	Lin. Acc.	Z	0.712	0.721	0.476	0.406
R	330	1	C7/T1	Lin. Acc.	X	0.616	0.780	0.616	0.687
R	330	1	C7/T1	Lin. Acc.	Y	0.718	0.709	0.474	0.509
R	330	1	C7/T1	Lin. Acc.	Z	0.949	1.069	0.215	0.212

R	330	2.5	Head	Ang. Vel.	X	1.950	1.271	0.212	0.226
R	330	2.5	Head	Ang. Vel.	Y	1.166	1.952	0.300	0.241
R	330	2.5	Head	Ang. Vel.	Z	0.949	0.628	0.177	0.438
R	330	2.5	Head	Lin. Acc.	X	1.183	1.692	0.323	0.300
R	330	2.5	Head	Lin. Acc.	Y	1.204	0.931	0.454	0.514
R	330	2.5	Head	Lin. Acc.	Z	0.744	0.807	0.372	0.313
R	330	2.5	C7/T1	Lin. Acc.	X	0.797	0.693	0.555	0.545
R	330	2.5	C7/T1	Lin. Acc.	Y	0.476	0.559	0.520	0.489
R	330	2.5	C7/T1	Lin. Acc.	Z	0.497	0.474	0.415	0.445
B	0	1	Head	Ang. Vel.	X	0.355	0.277	0.142	0.135
B	0	1	Head	Ang. Vel.	Y	1.000	0.431	0.695	0.784
B	0	1	Head	Ang. Vel.	Z	0.470	0.442	0.356	0.239
B	0	1	Head	Lin. Acc.	X	0.867	0.538	0.766	0.790
B	0	1	Head	Lin. Acc.	Y	0.494	0.284	0.246	0.190
B	0	1	Head	Lin. Acc.	Z	1.432	0.880	0.305	0.325
B	0	1	C7/T1	Lin. Acc.	X	1.127	0.733	0.647	0.749
B	0	1	C7/T1	Lin. Acc.	Y	0.382	0.226	0.221	0.534
B	0	1	C7/T1	Lin. Acc.	Z	1.671	0.996	0.233	0.228
B	0	2.5	Head	Ang. Vel.	X	2.205	0.642	0.081	0.269
B	0	2.5	Head	Ang. Vel.	Y	1.526	1.702	0.501	0.365
B	0	2.5	Head	Ang. Vel.	Z	1.259	0.570	0.142	0.144
B	0	2.5	Head	Lin. Acc.	X	1.858	1.893	0.541	0.318
B	0	2.5	Head	Lin. Acc.	Y	1.462	0.671	0.284	0.230
B	0	2.5	Head	Lin. Acc.	Z	1.895	1.905	0.370	0.311
B	0	2.5	C7/T1	Lin. Acc.	X	1.655	0.907	0.496	0.579
B	0	2.5	C7/T1	Lin. Acc.	Y	0.437	0.298	0.291	0.495
B	0	2.5	C7/T1	Lin. Acc.	Z	1.209	1.342	0.343	0.310
B	330	1	Head	Ang. Vel.	X	1.095	0.942	0.338	0.292
B	330	1	Head	Ang. Vel.	Y	0.808	0.825	0.648	0.633
B	330	1	Head	Ang. Vel.	Z	0.786	0.626	0.086	0.204
B	330	1	Head	Lin. Acc.	X	1.220	1.216	0.632	0.553
B	330	1	Head	Lin. Acc.	Y	1.676	1.122	0.397	0.412
B	330	1	Head	Lin. Acc.	Z	0.889	0.560	0.388	0.395
B	330	1	C7/T1	Lin. Acc.	X	0.865	0.675	0.611	0.726
B	330	1	C7/T1	Lin. Acc.	Y	0.850	0.721	0.405	0.521
B	330	1	C7/T1	Lin. Acc.	Z	0.963	0.542	0.256	0.215
B	330	2.5	Head	Ang. Vel.	X	1.204	1.224	0.439	0.217
B	330	2.5	Head	Ang. Vel.	Y	1.185	1.990	0.396	0.247
B	330	2.5	Head	Ang. Vel.	Z	0.861	0.505	0.156	0.424
B	330	2.5	Head	Lin. Acc.	X	1.175	1.051	0.482	0.414
B	330	2.5	Head	Lin. Acc.	Y	1.238	0.931	0.510	0.479
B	330	2.5	Head	Lin. Acc.	Z	0.768	0.898	0.345	0.342
B	330	2.5	C7/T1	Lin. Acc.	X	0.863	0.822	0.536	0.577
B	330	2.5	C7/T1	Lin. Acc.	Y	0.480	0.422	0.589	0.631
B	330	2.5	C7/T1	Lin. Acc.	Z	0.531	0.783	0.360	0.389

TABLE AII
BRS AND ISO SCORES FOR ALL EXCURSIONS.

Muscle Tone	PDOF (°)	Pulse (g)	Location	Signal	Direction	Female BRS	Male BRS	Female ISO	Male ISO
R	0	1	Head	CG	X	1.728	1.602	0.448	0.282
R	0	1	Head	CG	Y	0.374	0.429	0.393	0.423
R	0	1	Head	CG	Z	1.581	1.839	0.266	0.156
R	0	1	Shoulder	L	X	0.611	0.612	0.425	0.652
R	0	1	Shoulder	L	Y	1.505	1.282	0.362	0.213
R	0	1	Shoulder	L	Z	0.312	0.732	0.590	0.265
R	0	1	Shoulder	R	X	0.300	0.689	0.664	0.614
R	0	1	Shoulder	R	Y	0.436	0.644	0.222	0.228
R	0	1	Shoulder	R	Z	0.509	0.715	0.460	0.163
R	0	1	Elbow	L	X	0.668	0.791	0.388	0.418
R	0	1	Elbow	L	Y	0.290	0.581	0.469	0.181
R	0	1	Elbow	L	Z	1.251	1.157	0.209	0.213
R	0	1	Elbow	R	X	0.563	1.301	0.458	0.344
R	0	1	Elbow	R	Y	1.176	0.821	0.175	0.233
R	0	1	Elbow	R	Z	1.382	1.195	0.203	0.196
R	0	1	Hip	L	X	1.356	1.322	0.486	0.314
R	0	1	Hip	L	Y	0.607	0.588	0.364	0.208
R	0	1	Hip	L	Z	1.250	0.909	0.271	0.388
R	0	1	Hip	R	X	1.770	1.351	0.232	0.251
R	0	1	Hip	R	Y	0.259	0.114	0.306	0.627
R	0	1	Hip	R	Z	0.674	1.059	0.153	0.165
R	0	1	Knee	L	X	2.372	-	0.387	-
R	0	1	Knee	L	Y	0.314	-	0.300	-
R	0	1	Knee	L	Z	1.825	-	0.333	-
R	0	1	Knee	R	X	2.495	1.430	0.360	0.282
R	0	1	Knee	R	Y	0.516	0.862	0.165	0.158
R	0	1	Knee	R	Z	1.508	1.489	0.247	0.135
R	0	2.5	Head	CG	X	1.012	1.596	0.603	0.481
R	0	2.5	Head	CG	Y	0.671	0.693	0.485	0.484
R	0	2.5	Head	CG	Z	0.553	0.378	0.512	0.510
R	0	2.5	Shoulder	L	X	0.737	1.195	0.703	0.689
R	0	2.5	Shoulder	L	Y	2.270	1.327	0.169	0.338
R	0	2.5	Shoulder	L	Z	1.319	1.609	0.233	0.194
R	0	2.5	Shoulder	R	X	0.326	1.139	0.807	0.720
R	0	2.5	Shoulder	R	Y	0.703	1.027	0.207	0.173
R	0	2.5	Shoulder	R	Z	1.119	1.690	0.168	0.160
R	0	2.5	Elbow	L	X	0.909	1.302	0.599	0.607
R	0	2.5	Elbow	L	Y	0.547	0.949	0.193	0.232
R	0	2.5	Elbow	L	Z	1.890	1.841	0.296	0.289
R	0	2.5	Elbow	R	X	0.463	1.358	0.729	0.581
R	0	2.5	Elbow	R	Y	1.137	0.975	0.172	0.239
R	0	2.5	Elbow	R	Z	1.734	1.661	0.166	0.246
R	0	2.5	Hip	L	X	1.240	1.979	0.477	0.421
R	0	2.5	Hip	L	Y	1.474	0.614	0.380	0.257
R	0	2.5	Hip	L	Z	1.012	0.955	0.292	0.319
R	0	2.5	Hip	R	X	0.737	1.595	0.686	0.506
R	0	2.5	Hip	R	Y	0.520	0.372	0.535	0.354

R	0	2.5	Hip	R	Z	1.100	0.502	0.271	0.486
R	0	2.5	Knee	L	X	1.191	-	0.517	-
R	0	2.5	Knee	L	Y	0.477	-	0.234	-
R	0	2.5	Knee	L	Z	0.878	-	0.665	-
R	0	2.5	Knee	R	X	0.798	1.320	0.692	0.642
R	0	2.5	Knee	R	Y	0.351	0.282	0.251	0.292
R	0	2.5	Knee	R	Z	1.466	1.780	0.465	0.469
R	330	1	Head	CG	X	0.736	2.850	0.540	0.256
R	330	1	Head	CG	Y	1.512	0.413	0.603	0.884
R	330	1	Head	CG	Z	1.429	1.634	0.212	0.241
R	330	1	Shoulder	L	X	1.094	1.334	0.331	0.657
R	330	1	Shoulder	L	Y	0.448	0.140	0.778	0.959
R	330	1	Shoulder	L	Z	0.468	1.527	0.427	0.119
R	330	1	Shoulder	R	X	0.195	2.153	0.443	0.259
R	330	1	Shoulder	R	Y	2.158	1.389	0.578	0.703
R	330	1	Shoulder	R	Z	2.402	1.073	0.226	0.337
R	330	1	Elbow	L	X	1.083	1.834	0.473	0.522
R	330	1	Elbow	L	Y	1.696	2.749	0.349	0.178
R	330	1	Elbow	L	Z	1.439	2.417	0.114	0.103
R	330	1	Elbow	R	X	0.508	1.728	0.408	0.255
R	330	1	Elbow	R	Y	0.584	1.257	0.424	0.283
R	330	1	Elbow	R	Z	1.332	0.465	0.282	0.540
R	330	1	Hip	L	X	-	1.492	-	0.160
R	330	1	Hip	L	Y	-	2.041	-	0.280
R	330	1	Hip	L	Z	-	1.144	-	0.217
R	330	1	Hip	R	X	-	1.940	-	0.132
R	330	1	Hip	R	Y	-	0.288	-	0.762
R	330	1	Hip	R	Z	-	3.442	-	0.079
R	330	1	Knee	L	X	1.239	-	0.268	-
R	330	1	Knee	L	Y	1.097	-	0.218	-
R	330	1	Knee	L	Z	0.589	-	0.325	-
R	330	1	Knee	R	X	1.425	1.780	0.174	0.288
R	330	1	Knee	R	Y	2.170	1.495	0.191	0.360
R	330	1	Knee	R	Z	1.267	0.760	0.241	0.487
R	330	2.5	Head	CG	X	0.778	1.626	0.589	0.369
R	330	2.5	Head	CG	Y	0.425	0.651	0.949	0.789
R	330	2.5	Head	CG	Z	0.552	0.515	0.571	0.495
R	330	2.5	Shoulder	L	X	1.258	0.727	0.546	0.768
R	330	2.5	Shoulder	L	Y	1.740	1.004	0.518	0.539
R	330	2.5	Shoulder	L	Z	1.485	2.156	0.162	0.133
R	330	2.5	Shoulder	R	X	0.489	0.782	0.711	0.675
R	330	2.5	Shoulder	R	Y	0.842	0.966	0.881	0.735
R	330	2.5	Shoulder	R	Z	0.889	1.054	0.429	0.360
R	330	2.5	Elbow	L	X	1.764	0.945	0.518	0.708
R	330	2.5	Elbow	L	Y	1.386	1.311	0.710	0.613
R	330	2.5	Elbow	L	Z	2.529	2.667	0.163	0.166
R	330	2.5	Elbow	R	X	0.560	1.390	0.718	0.408
R	330	2.5	Elbow	R	Y	1.522	0.901	0.438	0.220
R	330	2.5	Elbow	R	Z	1.827	1.486	0.383	0.406
R	330	2.5	Hip	L	X	1.402	1.641	0.381	0.391
R	330	2.5	Hip	L	Y	0.274	0.574	0.778	0.533

R	330	2.5	Hip	L	Z	0.817	0.663	0.240	0.305
R	330	2.5	Hip	R	X	1.429	1.227	0.332	0.471
R	330	2.5	Hip	R	Y	0.174	0.950	0.854	0.527
R	330	2.5	Hip	R	Z	1.207	1.862	0.271	0.197
R	330	2.5	Knee	L	X	1.465	2.160	0.443	0.435
R	330	2.5	Knee	L	Y	1.773	1.106	0.418	0.418
R	330	2.5	Knee	L	Z	0.564	0.669	0.590	0.539
R	330	2.5	Knee	R	X	1.450	1.899	0.457	0.406
R	330	2.5	Knee	R	Y	2.162	1.064	0.315	0.380
R	330	2.5	Knee	R	Z	2.221	0.985	0.403	0.580
B	0	1	Head	CG	X	0.470	0.388	0.890	0.787
B	0	1	Head	CG	Y	0.456	1.211	0.088	0.100
B	0	1	Head	CG	Z	3.648	1.582	0.143	0.216
B	0	1	Shoulder	L	X	4.619	3.075	0.094	0.237
B	0	1	Shoulder	L	Y	0.460	1.059	0.537	0.299
B	0	1	Shoulder	L	Z	2.230	1.936	0.098	0.121
B	0	1	Shoulder	R	X	4.905	3.284	0.125	0.259
B	0	1	Shoulder	R	Y	1.505	2.711	0.113	0.084
B	0	1	Shoulder	R	Z	2.310	2.653	0.082	0.085
B	0	1	Elbow	L	X	2.528	1.798	0.140	0.261
B	0	1	Elbow	L	Y	1.574	1.064	0.025	0.093
B	0	1	Elbow	L	Z	1.229	1.314	0.201	0.278
B	0	1	Elbow	R	X	3.928	1.829	0.071	0.242
B	0	1	Elbow	R	Y	0.566	1.196	0.067	0.032
B	0	1	Elbow	R	Z	1.846	2.297	0.163	0.211
B	0	1	Hip	L	X	2.116	2.325	0.271	0.236
B	0	1	Hip	L	Y	0.740	0.754	0.117	0.150
B	0	1	Hip	L	Z	0.356	0.287	0.240	0.437
B	0	1	Hip	R	X	1.168	1.622	0.277	0.268
B	0	1	Hip	R	Y	0.300	0.779	0.190	0.195
B	0	1	Hip	R	Z	0.613	0.708	0.140	0.301
B	0	1	Knee	L	X	1.473	-	0.284	-
B	0	1	Knee	L	Y	0.435	-	0.215	-
B	0	1	Knee	L	Z	0.628	-	0.143	-
B	0	1	Knee	R	X	1.071	1.557	0.326	0.294
B	0	1	Knee	R	Y	1.022	1.867	0.111	0.087
B	0	1	Knee	R	Z	0.491	1.810	0.219	0.091
B	0	2.5	Head	CG	X	1.508	1.003	0.550	0.448
B	0	2.5	Head	CG	Y	0.991	1.768	0.142	0.078
B	0	2.5	Head	CG	Z	1.471	0.609	0.401	0.458
B	0	2.5	Shoulder	L	X	6.142	2.772	0.117	0.250
B	0	2.5	Shoulder	L	Y	0.461	0.916	0.312	0.230
B	0	2.5	Shoulder	L	Z	1.030	1.341	0.184	0.188
B	0	2.5	Shoulder	R	X	4.980	3.789	0.236	0.255
B	0	2.5	Shoulder	R	Y	2.747	2.859	0.158	0.055
B	0	2.5	Shoulder	R	Z	1.889	2.250	0.171	0.126
B	0	2.5	Elbow	L	X	3.257	1.666	0.260	0.326
B	0	2.5	Elbow	L	Y	0.994	0.771	0.283	0.319
B	0	2.5	Elbow	L	Z	1.066	1.639	0.304	0.322
B	0	2.5	Elbow	R	X	4.789	2.304	0.229	0.331
B	0	2.5	Elbow	R	Y	1.816	0.819	0.088	0.142

B	0	2.5	Elbow	R	Z	1.359	3.583	0.309	0.254
B	0	2.5	Hip	L	X	0.375	0.456	0.776	0.692
B	0	2.5	Hip	L	Y	2.079	1.415	0.159	0.204
B	0	2.5	Hip	L	Z	0.360	0.433	0.233	0.395
B	0	2.5	Hip	R	X	0.650	0.649	0.625	0.635
B	0	2.5	Hip	R	Y	1.172	0.744	0.122	0.200
B	0	2.5	Hip	R	Z	0.588	1.154	0.417	0.181
B	0	2.5	Knee	L	X	0.392	-	0.798	-
B	0	2.5	Knee	L	Y	0.930	-	0.188	-
B	0	2.5	Knee	L	Z	0.414	-	0.674	-
B	0	2.5	Knee	R	X	0.841	0.727	0.510	0.624
B	0	2.5	Knee	R	Y	0.877	0.811	0.162	0.327
B	0	2.5	Knee	R	Z	0.330	0.759	0.743	0.519
B	330	1	Head	CG	X	0.364	1.533	0.866	0.353
B	330	1	Head	CG	Y	1.516	1.526	0.624	0.636
B	330	1	Head	CG	Z	1.605	0.298	0.332	0.344
B	330	1	Shoulder	L	X	5.820	4.564	0.053	0.147
B	330	1	Shoulder	L	Y	1.845	1.260	0.318	0.516
B	330	1	Shoulder	L	Z	0.537	2.406	0.613	0.262
B	330	1	Shoulder	R	X	3.215	1.077	0.280	0.316
B	330	1	Shoulder	R	Y	1.321	0.916	0.562	0.631
B	330	1	Shoulder	R	Z	3.949	3.092	0.129	0.243
B	330	1	Elbow	L	X	4.023	1.765	0.173	0.353
B	330	1	Elbow	L	Y	1.681	1.853	0.301	0.392
B	330	1	Elbow	L	Z	1.774	3.470	0.269	0.198
B	330	1	Elbow	R	X	0.669	1.812	0.435	0.346
B	330	1	Elbow	R	Y	0.766	0.891	0.294	0.534
B	330	1	Elbow	R	Z	0.952	1.371	0.294	0.320
B	330	1	Hip	L	X	-	1.244	-	0.141
B	330	1	Hip	L	Y	-	1.077	-	0.362
B	330	1	Hip	L	Z	-	1.906	-	0.151
B	330	1	Hip	R	X	-	2.885	-	0.126
B	330	1	Hip	R	Y	-	0.865	-	0.316
B	330	1	Hip	R	Z	-	4.467	-	0.084
B	330	1	Knee	L	X	0.924	-	0.278	-
B	330	1	Knee	L	Y	0.555	-	0.502	-
B	330	1	Knee	L	Z	0.259	-	0.287	-
B	330	1	Knee	R	X	0.899	1.431	0.213	0.255
B	330	1	Knee	R	Y	1.079	1.320	0.402	0.446
B	330	1	Knee	R	Z	0.369	0.700	0.489	0.404
B	330	2.5	Head	CG	X	1.293	1.277	0.559	0.385
B	330	2.5	Head	CG	Y	1.622	1.316	0.634	0.599
B	330	2.5	Head	CG	Z	0.974	0.491	0.487	0.544
B	330	2.5	Shoulder	L	X	4.235	3.535	0.109	0.188
B	330	2.5	Shoulder	L	Y	2.352	1.411	0.329	0.416
B	330	2.5	Shoulder	L	Z	1.564	1.669	0.305	0.176
B	330	2.5	Shoulder	R	X	2.040	1.337	0.255	0.297
B	330	2.5	Shoulder	R	Y	1.464	0.848	0.609	0.648
B	330	2.5	Shoulder	R	Z	1.564	0.985	0.222	0.451
B	330	2.5	Elbow	L	X	3.913	2.365	0.187	0.300
B	330	2.5	Elbow	L	Y	1.361	1.881	0.392	0.475

B	330	2.5	Elbow	L	Z	1.332	1.640	0.257	0.255
B	330	2.5	Elbow	R	X	1.268	1.497	0.412	0.331
B	330	2.5	Elbow	R	Y	2.202	1.849	0.444	0.268
B	330	2.5	Elbow	R	Z	0.626	1.152	0.489	0.435
B	330	2.5	Hip	L	X	0.652	0.976	0.626	0.393
B	330	2.5	Hip	L	Y	0.948	1.617	0.660	0.248
B	330	2.5	Hip	L	Z	1.207	0.565	0.205	0.314
B	330	2.5	Hip	R	X	1.162	0.742	0.392	0.610
B	330	2.5	Hip	R	Y	0.804	0.867	0.632	0.524
B	330	2.5	Hip	R	Z	0.603	1.473	0.253	0.180
B	330	2.5	Knee	L	X	0.568	1.400	0.730	0.425
B	330	2.5	Knee	L	Y	1.251	1.835	0.444	0.210
B	330	2.5	Knee	L	Z	0.834	0.727	0.331	0.554
B	330	2.5	Knee	R	X	0.546	1.815	0.668	0.416
B	330	2.5	Knee	R	Y	1.023	1.257	0.574	0.568
B	330	2.5	Knee	R	Z	0.443	0.617	0.680	0.707